

# ELMoE-3D: Leveraging Intrinsic Elasticity of MoE for Hybrid-Bonding-Enabled Self-Speculative Decoding in On-Premises Serving

Yuseon Choi  
KAIST  
Daejeon, Republic of Korea  
yuseon.choi@kaist.ac.kr

Jingu Lee  
KAIST  
Daejeon, Republic of Korea  
guya102@kaist.ac.kr

Jungjun Oh  
KAIST  
Daejeon, Republic of Korea  
ojj1245@kaist.ac.kr

Sunjoon Whang  
KAIST  
Daejeon, Republic of Korea  
sjwhang@kaist.ac.kr

Byeongcheol Kim  
Samsung Electronics  
Hwasung, Republic of Korea  
bc27.kim@samsung.com

Minsung Kim  
KAIST  
Daejeon, Republic of Korea  
minsung.kim@kaist.ac.kr

Hoi-Jun Yoo  
KAIST  
Daejeon, Republic of Korea  
hjyoo@kaist.ac.kr

Sangjin Kim  
GIST  
Gwangju, Republic of Korea  
sangjinkim@gist.ac.kr

## Abstract

Mixture-of-Experts (MoE) models have become the dominant architecture for large-scale language models, yet on-premises serving remains fundamentally memory-bound as batching turns sparse per-token compute into dense memory activation. Memory-centric architectures (PIM, NMP) improve bandwidth but leave compute underutilized under MoE’s low arithmetic intensity at high batch sizes. Speculative decoding (SD) trades idle compute for fewer target invocations, yet verification must load experts even for rejected tokens, severely limiting its benefit in MoE especially at low batch sizes. We propose ELMoE-3D, a hybrid-bonding (HB)-based HW-SW co-designed framework that unifies cache-based acceleration and speculative decoding to offer overall speedup across batch sizes. We identify two intrinsic elasticity axes of MoE—expert and bit—and jointly scale them to construct Elastic Self-Speculative Decoding (Elastic-SD), which serves as both an expert cache and a strongly aligned self-draft model accelerated by high HB bandwidth. Our LSB-augmented bit-sliced architecture exploits inherent redundancy in bit-slice representations to natively support bit-nested execution. On our 3D-stacked hardware, ELMoE-3D achieves an average 6.6× speedup and 4.4× energy efficiency gain over naïve MoE serving on xPU across batch sizes 1–16, and delivers 2.2× speedup and 1.4× energy efficiency gain over the best-performing prior accelerator baseline.

## Keywords

Near Memory Processing, Hybrid-Bonding, Mixture-of-Experts, Speculative Decoding, On-premises Serving

## 1 Introduction

Transformer-based large language models (LLMs) have achieved remarkable success in natural language processing, under the scaling law [27]. Increasing parameter count improves performance but proportionally increases computational cost. Mixture-of-Experts (MoE)

addresses this challenge by sparsely gating FFN layers, increasing model capacity while maintaining computational efficiency [56]. Today, MoE architectures are widely adopted across model scales, from compact edge-deployable variants to server-scale deployments, making efficient MoE inference acceleration essential for modern NLP systems.

Recent MoE models around 30B parameters [10, 47, 59, 66]—are emerging as attractive candidates for on-premises serving, where data privacy, low latency, and independence from cloud infrastructure are prioritized [20]. Personal AI workstations such as NVIDIA DGX Spark and Apple Mac Studio [1, 46] can host such models locally, but serving MoE poses a fundamental memory bottleneck. Since activated experts are independently selected per token, batching or prefill operations activate nearly all experts collectively. Although computation remains sparse per token, memory activation becomes effectively dense across the batch [2, 70].

To address this bandwidth bottleneck, memory-centric architectures have been explored. PIM [19, 70] and NMP [35, 48] alleviate raw bandwidth limitations, but MoE’s low arithmetic intensity at expert layers limits their compute utilization. 3D-IC with hybrid bonding [67, 69] places high-bandwidth memory directly above the compute die, but its limited capacity leads to significant cache hit rate degradation under batching. Both approaches provide hardware-level relief but do not address the fundamental algorithm–architecture mismatch inherent in MoE inference.

Speculative decoding (SD) [34] offers an algorithmic complement by drafting multiple tokens and verifying them in a single forward pass, effectively raising arithmetic intensity. However, SD is misaligned with MoE’s sparse activation: verification must load experts for all drafted tokens including rejected ones, inflating memory traffic—especially at low batch sizes where verify-phase expert activation far exceeds AR decoding [3, 16, 21, 41, 54]. Prior 3D-IC-based approaches [11, 71] reduce draft cost but still suffer from high verification overhead, as models small enough to fit in the caches [15, 38] exhibit low acceptance lengths.

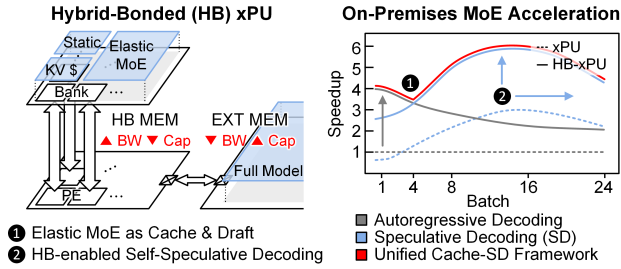


Figure 1: Overview of ELMoE-3D.

To address this, we architect a hybrid-bonding-based xPU system that unifies cache-based AR acceleration at low batch sizes and speculative decoding at high batch sizes within a single framework, as illustrated in Fig. 1. The key insight is that a subset of MoE parameters can serve as a draft model in self speculative decoding. This is enabled by two orthogonal axes of elasticity. Expert elasticity [7, 41, 57] exploits heavy-tailed routing for hardware-aware expert selection, while bit elasticity [28, 31, 44, 51] leverages nested quantization to scale precision on demand. Together, these enable a unified cache-draft mapping that effectively utilizes high-bandwidth but capacity-limited hybrid-bonded memory across the full batch size range.

Building on these insights, we propose **ELMoE-3D**, a hybrid-bonding-based HW-SW co-designed MoE inference framework. Our contributions are as follows:

- **Elastic Self-Speculative Decoding (Elastic-SD):** We propose expert throttling that caches MSB slices of hot experts in residual HB memory, constructing a self-draft model with high target alignment while simultaneously accelerating verification.
- **LSB-Augmented Bit-Sliced Architecture:** We repurpose the sign-extension overhead inherent in bit-sliced MAC as implicit LSB rounding, enabling bit-nested quantization without additional hardware cost.
- **Elasticity-Aware Execution Engine:** We design a phase-aware execution flow that schedules mixed-precision computation across HB and external memory tiers to efficiently serve each SD phase.

## 2 Background

### 2.1 Mixture-of-Experts (MoE)

As shown in Fig. 2 (left), Mixture-of-Experts (MoE) is a model architecture built on sparsely gated FFN layers, where each token selectively activates top- $k$  experts based on routing scores, scaling parameter capacity while keeping per-token computation bounded [56]. The outputs of selected experts are combined via a weighted sum using the corresponding gating scores.

Prior works exploit expert locality through prefetching and caching for efficient MoE inference. Pregated MoE [23] leverages temporal locality across decoding steps to prefetch experts and hide memory latency. Caching strategies [65] keep frequently used experts in faster memory based on input context or task characteristics.

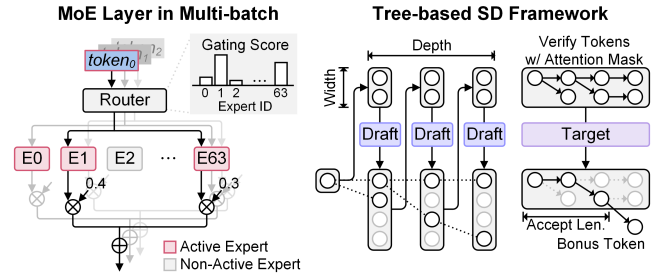


Figure 2: Mixture-of-Experts and Speculative Decoding.

More recently, several works have observed that routing scores follow a heavy-tailed distribution, implying that strict top- $k$  selection is not always necessary for maintaining model quality [7, 57, 62]. These approaches reduce memory access by substituting or restricting expert choices while preserving performance.

However, such locality- and sparsity-driven optimizations become less effective under batching. Because expert selection is independent across tokens, different tokens in a batch activate different experts simultaneously. Although per-token computation remains sparse, memory activation becomes effectively dense at the batch level [16, 41, 68], creating a severe bandwidth bottleneck in memory-constrained on-premise systems.

### 2.2 Speculative Decoding (SD)

Speculative Decoding (SD) [36–38] accelerates autoregressive generation by using a lightweight draft model to propose multiple token candidates, which are verified by the target model in a single forward pass, as illustrated in Fig. 2 (right). SD is effective in memory-bound systems, where batching can utilize otherwise idle compute to generate more tokens per step.

Recent approaches adopt a tree-based framework [36]. The draft model expands a token tree by iteratively batching width- $w$  candidates over  $d$  depth steps. Candidate paths are scored, and a subset of top-scoring nodes is selected as *verify tokens* and verified via tree attention. The number of consecutively accepted tokens is defined as the *accept length*, and additional *bonus tokens* is generated. The overall speedup can be expressed as:

$$\text{speedup} = \frac{(1 + \text{accepted length}) \cdot \text{latency}_{\text{autoregressive}}}{d \cdot \text{latency}_{\text{draft}} + \text{latency}_{\text{verify}}}$$

SD methods can be categorized into *independent drafting* and *self-drafting*. Independent methods use a separate draft model. For example, EAGLE3 [38] employs a lightweight head distilled from the target model, while Small Language Models (SLM)-SD [15] instead use a smaller model from the same family. They achieve strong performance with minimal draft cost, but suffer from weak target alignment and cannot share parameters or KV cache, duplicating storage for both models.

In contrast, self-speculative decoding (Self-SD) constructs the draft model as a subset or approximation of the target model [14]. LayerSkip [12] and Early-Exit [39] methods use partial layers with a trade-off between draft cost and acceptance ratio, often requiring additional training. Quantization-based Self-SD [14, 60, 61] achieves higher acceptance lengths at comparable cost without extra training,

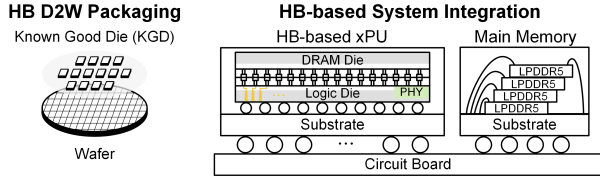


Figure 3: D2W hybrid bonding process and system integration.

though effectiveness degrades below 3-bit precision, making 4-bit the practical lower bound.

### 2.3 3D-IC and Hybrid Bonding (HB)

Three-dimensional integrated circuits (3D-ICs) stack multiple dies vertically, overcoming planar bandwidth limitations. Hybrid Bonding (HB) [32, 63, 69] directly joins copper pads and dielectric without bumps, achieving sub- $10\mu\text{m}$  pitch and I/O densities several hundred times greater than conventional micro-bump approaches. Among HB processes, Die-to-Wafer (D2W) [22] bonds individual Known Good Dies (KGDs) onto a wafer, enabling heterogeneous die sizes and process nodes with high yield, so that system specification can be tailored to workload requirements. Figure 3 shows the D2W hybrid bonding process and the resulting system architecture. DRAM dies are directly stacked on the logic die via HB, while off-package LPDDR5 [25] serves residual capacity, forming a hierarchical memory system. The on-die DRAM provides TB/s-class bandwidth, and the large bandwidth gap between HB and LPDDR5 naturally lends itself to a caching mechanism [64, 69], where frequently accessed data reside on-die and the rest are fetched from LPDDR5 on demand.

## 3 Motivation

### 3.1 Low Arithmetic Intensity in MoE Serving

In LLM inference, arithmetic intensity (AI) of dense layers scales linearly with batch size due to weight sharing across tokens. In contrast, MoE expert layers process only a subset of tokens, and their effective AI scales with  $bs \times \lambda$  ( $\lambda = N_{\text{active}}/N_{\text{total}}$ ), rather than  $bs$ . Consequently, even at large batch sizes, expert layers remain memory-bound while dominating inference latency due to their large weight size, as shown in Fig. 4(a).

Prior memory-centric architectures such as PIM and NMP provide high internal bandwidth but limited compute throughput. At small batch sizes this suffices, but as batch size grows, the increased expert activation exceeds their internal processing capability, forcing workload offloading to the host accelerator through the narrow external interconnect [19]. This external bandwidth then becomes the new bottleneck, negating the internal bandwidth advantage.

This limitation motivates a unified HW-SW approach that increases effective arithmetic intensity. Speculative decoding achieves this by batching draft and verify tokens, enabling the system to better utilize available bandwidth and achieve proportional latency reduction.

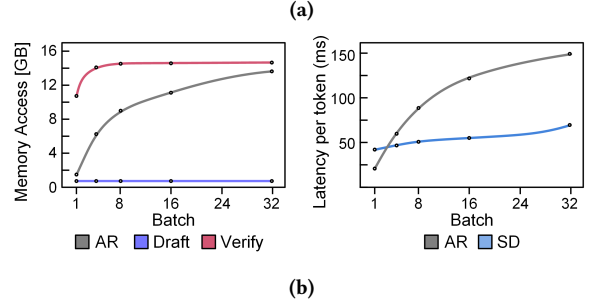
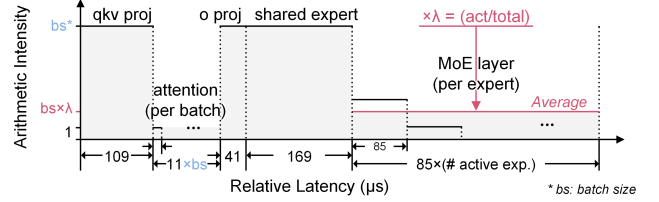


Figure 4: (a) Arithmetic intensity of MoE serving (DeepSeek-V2-Lite). (b) Misalignment between MoE and SD (Eagle3).

### 3.2 Misalignment between MoE and SD

Speculative Decoding (SD) improves utilization by drafting multiple tokens and verifying them in a single forward pass. However, in MoE models, verification introduces a fundamental inefficiency: experts are activated for all drafted tokens, including those that are ultimately rejected. As shown in Fig. 4(b) (left), this leads to a substantial increase in the number of activated experts compared to autoregressive (AR) decoding.

This mismatch leads to behavior that varies with batch size (Fig. 4(b), right). At low batch sizes, SD becomes inefficient due to excessive expert activation during verification. At high batch sizes, the effective token count from SD verification pushes expert layers into the compute-bound region, limiting SD benefit.

Prior 3D-IC-based approaches [11, 71] mitigate draft cost by placing draft models on stacked memory, but cache-fitting models suffer from low acceptance lengths, and parameter heterogeneity reduces effective cache capacity, leaving verification cost as the dominant bottleneck.

Therefore, effective MoE serving requires a fundamentally different approach: a self-speculative draft model that fits within HB’s limited capacity, maintains high alignment with the target MoE model, and shares the KV cache. This necessitates a tightly coupled HW-SW co-design over 3D-IC platforms.

### 3.3 Intrinsic Elasticity of MoE

To satisfy these requirements, we exploit two independent axes of elasticity inherent in MoE.

*Expert Elasticity.* MoE experts are trained in a mutually exclusive manner, preserving functionality at the expert level. This enables routing to be restricted to a hardware-aware subset without severe degradation, unlike dimension pruning in dense models. As shown in Fig. 5(a) left, we implement this via *expert throttling*, limiting each token to a predefined hot-expert subset while preserving routing score ordering. The heavy-tailed distribution of routing scores

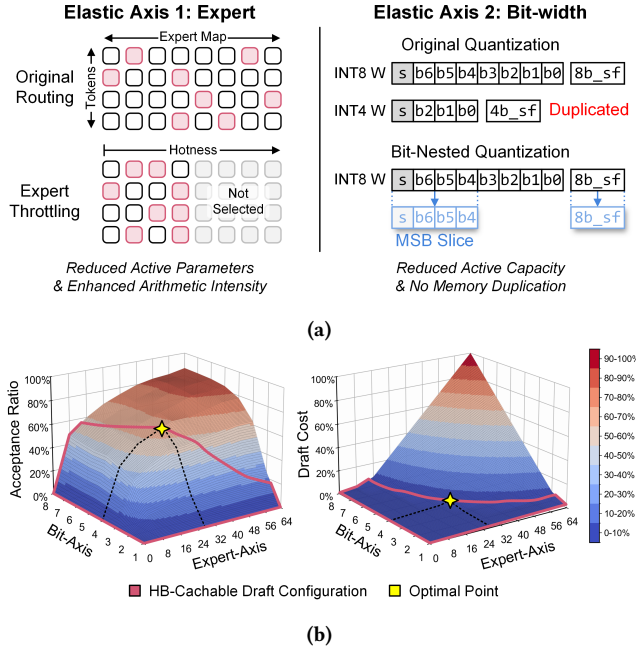


**Figure 5: (a) Expert and bit elasticity axes of MoE. (b) Acceptance ratio and draft cost under joint axis scaling.**

further enables flexible selection among experts with similar scores near the top- $k$  boundary, suppressing the total number of activated experts and preventing dense memory activation.

**Bit-width Elasticity.** Among elasticity axes, bit-width scaling best preserves weight vector direction, which is advantageous for draft-target alignment. However, conventional integer quantization uses different scaling factors per bit-width, requiring duplicated storage for multiple precisions. As depicted in Fig. 5(a) right, bit-nested quantization resolves this by designing the MSB slice of an INT8 weight to be itself a valid low-bit weight, enabling precision switching via simple bit truncation without memory duplication.

**Two-Axis Exploration.** As shown in Fig. 5(b), jointly exploring both axes reveals that acceptance ratio remains robust even as either axis is scaled down to reduce draft cost. The red region delineates HB-cacheable configurations, and the yellow star marks the optimal point minimizing draft cost while maintaining high acceptance ratio. This demonstrates that combining both elasticity axes yields a self-speculative draft model with high acceptance and low cost under HB constraints.

## 4 Proposed ELMoE-3D Architecture

### 4.1 Design Overview

ELMoE-3D is a hardware-software co-designed framework for efficient MoE inference on hybrid-bonding-based xPU. It targets on-premise serving with batch sizes of 1 to 16, supporting  $\sim 30\text{B}$ -scale MoE models under INT8 G32 symmetric quantization with elastic self-speculative decoding.

**Overall Architecture.** Fig. 6 (left) illustrates the system, which comprises two heterogeneous memory tiers: 4 or 8GB hybrid-bonded

(HB) memory and 64GB LPDDR external (EXT) memory. Throughput and bandwidth scale with HB capacity. Each PE is paired with an HB bank for high-bandwidth local access, while external memory connects via a lower-bandwidth LPDDR PHY. PEs are organized into groups with aggregation links, and a streamlined interconnect circulates across PE groups.

**HB-based Microarchitecture Design.** In Fig. 6 (center), each PE fetches data from its HB bank via an HB controller and from external memory via the streamline. The PE includes 32KB WMEM and 32KB IOMEM, driving a  $16 \times 32 \times 32$  tensor PE array. A bit-sliced unit PE supports multi-precision weights (4–8 bit) with 8-bit activations. A vector processing unit (VPU) handles element-wise operations and non-GEMM workloads. Partial sums are accumulated through a 32-way adder tree and immediately scaled, fusing dequantization into the accumulation path.

**Logic Die Datapath and Control.** Fig. 6 (right) shows the datapath, where a memory controller orchestrates data flow from both tiers. HB data is routed to IOMEM and WMEM, while streamline data circulates across PE groups and is written to WMEM. The streamline enables high-bandwidth weight delivery, whereas the aggregation link supports flexible communication (e.g., all-to-all, all-reduce) via control logic with buffering, bypass, and accumulation support.

### 4.2 HB-enabled Elastic Self-SD

**Elastic-SD.** Elastic-SD leverages the remaining capacity of HB memory to host a draft model. A subset of experts is pre-selected based on hotness, sized to fit the available HB headroom. As discussed in Fig. 5(b), jointly exploring the expert and bit axes yields the optimal cost-acceptance trade-off. Accordingly, 4-bit MSB slices are adopted as the draft unit. Routing is then enforced exclusively within this subset throughout the entire draft phase. By confining expert access to HB-resident data, Elastic-SD eliminates external memory accesses during drafting, significantly reducing draft latency. As depicted in Fig. 7, the constraint holds across the batch, draft width, and all iterations up to the full draft depth. This means an originally preferred expert (e.g. Expert 6) may be unavailable, and the highest-scoring candidate within the subset (e.g. Expert 3) is selected instead. Because the selection still follows original routing scores without modification, draft quality is preserved.

**Expert Throttling.** Selecting experts by jointly trimming the expert and bit axes to match HB’s remaining capacity is what we term *throttling*. While different expert combinations would normally activate at every batch, width, and depth step, we observe that width and depth contexts largely overlap. Hotness-based selection therefore suffices to cover the full draft with a single fixed subset, avoiding per-step expert selection overhead and stabilizing memory access patterns. To compute hotness hardware-efficiently, we convert each original routing decision’s selected experts into one-hot vectors and accumulate them across preceding draft steps. This is possible only in a self-speculative decoding setting, where routing information is already available during the draft phase [61].

**Expert Pool Update.** The expert pool must be periodically refreshed, yet HB and external memory lack a direct link and the external bandwidth is limited, precluding on-demand loading. This

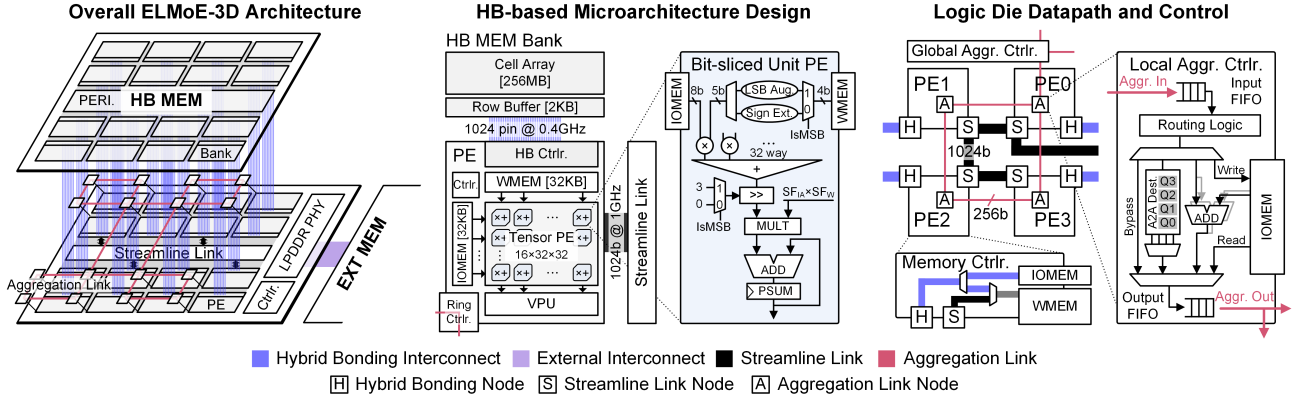


Figure 6: Overall architecture of ELMoE-3D.

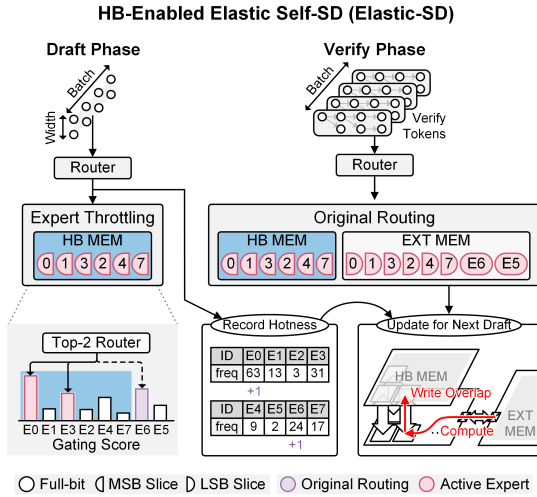


Figure 7: Elastic-SD execution flow.

is precisely why the next subset must be determined in advance. The accumulated one-hot vectors from the current draft phase identify the required experts before verification begins. During verification, expert data is sequentially fetched from external memory, and any piece belonging to the next-draft subset is simultaneously written into HB at the data-mapping granularity described in Section 5.1. The next draft model is thus transferred in overlap with verification compute at zero additional latency.

As a result, MSB slices alone provide a draft model with strong target alignment, while HB’s high-bandwidth capacity keeps the draft cost low. The bit-nested weight layout further allows verification data to be transferred in overlap, hiding the pool update cost. The overall execution flow is detailed in Algorithm 1.

### 4.3 LSB-Augmented Bit-Sliced Architecture for Bit-Nest Quantization

Bit-nest quantization enables a single representation to serve multiple bit precisions. However, under uniform quantization, each bit position contributes a different scaling factor to the final value, so naive bit truncation alone cannot preserve accuracy. Prior works

addressed this through quantization-aware-training (QAT) [44], non-uniform quantization (NUQ) [49, 51], or calibration-based post-training quantization (PTQ) [31], but these are difficult to apply in a plug-and-play manner. SliceMoE [7] proposed a calibration-free PTQ method that achieves bit nesting naturally: by truncating both the quantized weights and their per-group zero-points together under asymmetric quantization, each group adaptively retains a faithful approximation of the original data even after truncation. However, asymmetric weight quantization incurs additional metadata storage and computational overhead from the zero-point, making it inefficient for serving.

*Revisiting Bit-Slice Redundancy.* In a conventional bit-slice architecture [5, 6, 24, 26, 55], a signed 8-bit weight is split into two slices fed into the same signed $\times$ signed arithmetic unit. The LSB slice, originally unsigned, requires an auxiliary 1-bit zero-extension to become signed, while the MSB slice undergoes sign extension that carries no new information.

As shown in Fig.8, plain bit truncation shows the high clipping error such as [0, 15] error when truncating lower 4-bits. Rounding the MSB slice reduces this to  $[-8, 7]$ , but alters MSB values and creates a residual that no longer fits in the range of LSB slice. SIBIA [24] sacrifices full precision bit-width as 7 for this residual, NestQuant [53] stores a 5-bit residual (4+5=9 bits total), and Revolver [30] stores independently quantized residuals separately. In all cases, rounding trades additional memory footprint to reduce clipping error.

*LSB Augmentation.* Instead of sign-extending the MSB slice, we left-align the data and hardware a 1 at the LSB position of the 5-bit field during MSB-only operation (draft phase) and a 0 when combining with the full 8 bits (AR/verify phase). This effectively adds a half-unit offset to the MSB slice. As a result, 4-bit data is represented as a rounding approximation on the 8-bit scaling grid rather than a clipping approximation, preserving high accuracy. The hardware cost is a single multiplexer and its control signal—a micro-architectural compensation on the existing datapath.

Through this, we obtain a bit-nested draft model with high acceptance ratio at no additional memory footprint or hardware overhead beyond the baseline bit-slice architecture.

---

**Algorithm 1** HB-Aware Hybrid AR/SD Serving
 

---

**Require:** Batched tokens  $\mathcal{B}$ , Cached expert set  $C$ 
**Ensure:** Output tokens  $\mathcal{Y}$ 
**HB (on-chip):** DenseLayer, MSB( $C$ )

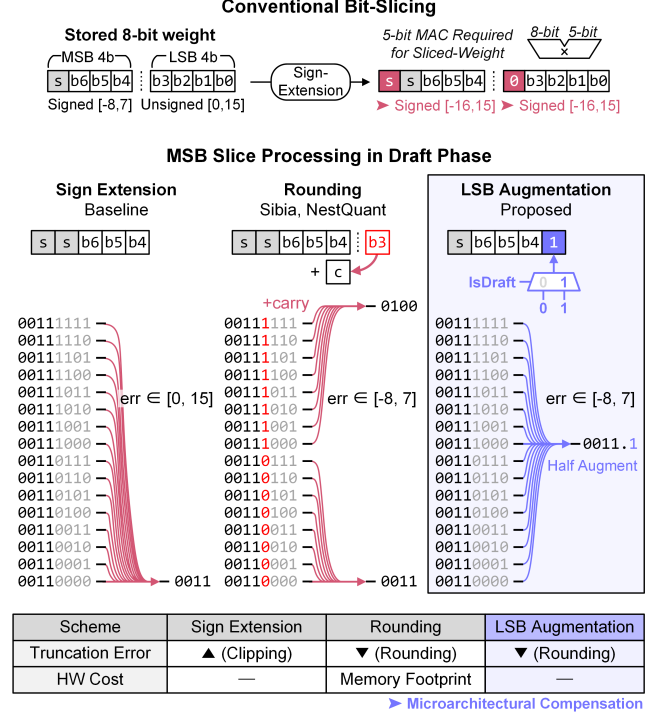
**EXT (off-chip):** LSB( $C$ ), uncached experts

```

1: if  $|\mathcal{B}| \geq \tau$  then
2:   for draft depth  $d$  do
3:      $x \leftarrow \text{EMBED}(\mathcal{B})$ 
4:     for layer  $\ell$  do
5:        $x \leftarrow \text{DENSELAYER}(x)$ 
6:        $\mathcal{G}_{\text{thr}} \leftarrow \text{TOPK}(\text{ROUTE}(x) | C)$ 
7:       for all  $e \in \text{Experts}[\mathcal{G}_{\text{thr}}]$  do
8:          $x \leftarrow x + e(x; \text{MSB}(\text{HB}[e]) \parallel 0)$ 
9:       end for
10:      RECORDHOTNESS()
11:    end for
12:     $\mathcal{B} \leftarrow \text{SAMPLE}(x)$ 
13:  end for
14:   $x \leftarrow \text{EMBED}(\mathcal{B})$ 
15:  for layer  $\ell$  do
16:     $x \leftarrow \text{DENSELAYER}(x)$ 
17:     $\mathcal{G} \leftarrow \text{TOPK}(\text{ROUTE}(x))$ 
18:    for all  $e \in \text{Experts}[\mathcal{G}]$  do
19:      if  $e \in C$  then
20:         $x \leftarrow x + e(x; \text{MSB}(\text{HB}[e]) \parallel 0)$ 
21:         $x \leftarrow x + e(x; \text{LSB}(\text{EXT}[e]))$ 
22:      else
23:         $x \leftarrow x + e(x; \text{EXT}[e])$ 
24:      end if
25:    end for
26:    UPDATECACHE(MSB( $e$ ))
27:  end for
28:   $\mathcal{Y} \leftarrow \text{SAMPLE}(\text{ACCEPT}(x))$ 
29: else
30:   $\mathcal{Y} \leftarrow \text{DECODE}(\mathcal{B})$ 
31: end if
32: return  $\mathcal{Y}$ 

```

▶ Speculative Decoding  
 ▶ Draft Phase  
 ▶ Expert Throttling  
 ▶ LSB Aug.  
 ▶ Verify Phase  
 ▶ Original Routing  
 ▶ LSB Aug.  
 ▶ Autoregressive Decoding


**Figure 8: Bit-nested quantization with the proposed LSB augmentation.**

**Phase-wise Data-Tensor Parallelism.** The distinct characteristics of HB and EXT memory necessitate different parallelization strategies. In HB, each bank-PE datapath carries distinct data, making Tensor Parallelism (TP) a natural fit, where weights are partitioned across PEs and activations are replicated across PEs. In contrast, EXT provides a fixed bandwidth through a shared interconnect, favoring Data Parallelism (DP), where weights are shared across PEs and activations are partitioned.

This choice is further aligned with the weight reuse patterns in the SD pipeline. In the Draft phase, routing is restricted to the HB-resident subset, and weight reuse scales with batch size and draft width. In the Verify phase, reuse scales with batch size and the number of verify tokens, which is typically much larger, resulting in significantly higher reuse. Accordingly, Draft employs HB-only TP to fully activate all bank-PE datapaths, while Verify combines HB-TP with EXT-DP to efficiently exploit both tiers.

## 5.2 Activation Communication Strategy

*MSB-LSB Weight Asynchronous Processing.*

**MSB-LSB Weight Asynchronous Processing.** Phase-wise parallelism processes MSB slices from HB using TP and LSB slices from EXT using DP. The two operations are executed in parallel only when the MSB slice resides in HB, enabling concurrent use of HB and EXT bandwidth. The key design question is the granularity at which results from the two slices should be synchronized.

As shown in Fig. 10(a), reconstructing full-precision weights by exchanging slices across PEs incurs communication cost proportional to the MSB slice size. In contrast, PSUM-level synchronization

## 5 ELMoE-3D Execution Engine

ELMoE-3D orchestrates data placement and computation across heterogeneous memory tiers to efficiently execute Elastic-SD. We first describe how memory characteristics guide parallelism decisions, then how computation is handled within the logic die.

### 5.1 Phase-wise Parallelism Exploitation

**Coupled vs. Decoupled Memory Characteristics.** As depicted in Fig. 9(a), HB memory connects each bank one-to-one with a PE via a dedicated datapath, making bandwidth and throughput *coupled*. Engaging more PEs with unique workloads proportionally increases usable bandwidth, while idle PEs leave their corresponding bandwidth unused. External memory streams data through a single shared interconnect, making bandwidth and throughput *decoupled*. Fig. 9(b) illustrates this on the system-level roofline. At partial PE utilization, the coupled HB roofline scales down in both axes, while the decoupled external roofline drops only in throughput. This asymmetry motivates phase-wise parallelism that matches each tier’s characteristics.

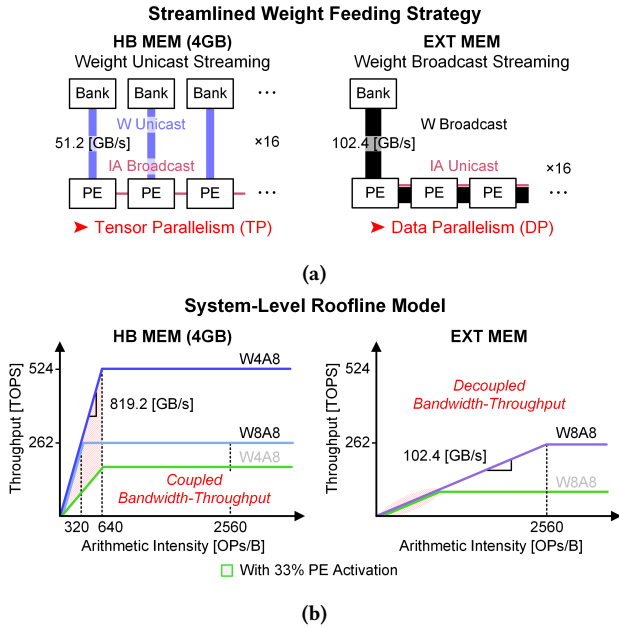


Figure 9: (a) Coupled (HB) and decoupled (EXT) memory characteristics. (b) System-level roofline.

allows each PE to compute MSB and LSB independently and exchange only partial sums, significantly reducing communication. The design goal is therefore to ensure that, across all batch sizes, communication latency does not exceed the LSB fetch time, so that execution is bounded by the slower EXT access.

Fig. 10(b) shows the execution timeline under worst-case communication. Following Stratum [48], the up, gate, and down projections are fused into a single expert. MSB and LSB slices are fetched concurrently from HB and EXT and processed in parallel by the PE array, while the VPU handles SiLU and element-wise operations after the gate projection. PSUM gather and scatter occur at projection boundaries, followed by a final reduction after the down projection. All communication is overlapped with memory access and computation, remaining off the critical path even under skewed expert activation.

Fused execution introduces a dependency between FFN1 (up-gate) and FFN2 (down), requiring PSUM synchronization. TP produces channel-wise PSUMs, whereas DP produces batch-wise outputs. In the gather stage, TP partial sums are concatenated along the output channel dimension and combined with DP outputs to reconstruct the full result. In the scatter stage, the result is redistributed to match the layout required by the next projection. PSUM synchronization and next-stage data preparation are naturally overlapped.

## 6 Implementation

Table 1 summarizes the ELMoE-3D system specification.

**Logic Die.** The logic die is synthesized using the ASAP7 7nm FinFET PDK [8] at 0.7V and 1.0GHz. Each PE contains a  $16 \times 32 \times 32$  bit-sliced MAC array composed of  $IA8 \times W5$  integer unit PEs. We evaluate two configurations that scale PE count with HB DRAM

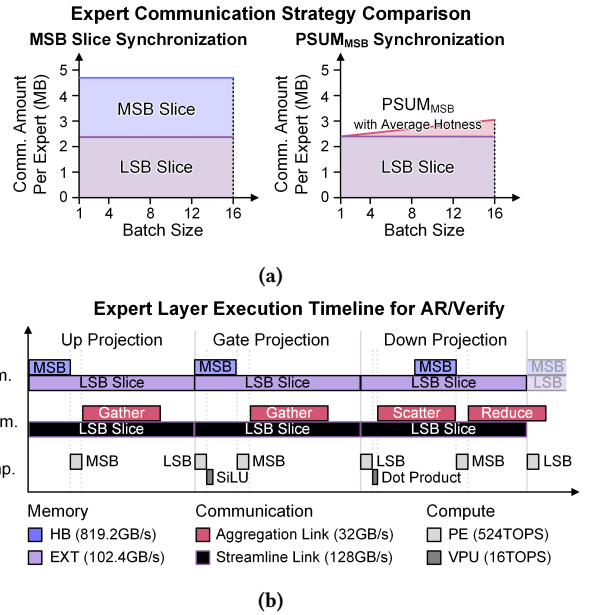


Figure 10: (a) On-chip communication volume per expert. (b) Expert-fused execution pipeline.

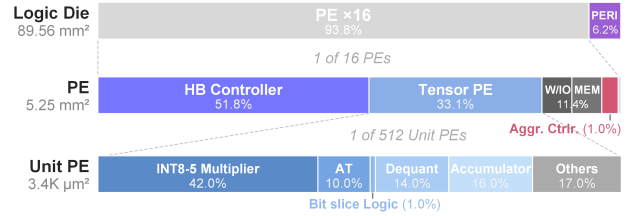


Figure 11: Logic die area breakdown (4GB configuration).

capacity, pairing 16 PEs with 4GB and 32 PEs with 8GB, proportionally scaling throughput and bandwidth. The aggregation link [33] (32GB/s) supports bypass, all-to-all, and accumulation for activation and PSUM transfer, while the streamline link (128GB/s) delivers external weight data directly into each PE's WMEM [43].

**Memory.** Each HB bank provides 51.2GB/s through 1024 pins at 0.4GHz, limited by the 2.5ns tCCD\_short constraint [17]. The read energy of 0.43 pJ/bit is scaled from [45] to 0.7V assuming quadratic voltage scaling. External memory uses LPDDR5-6400 [42] with 8 channels (x16), providing 102.4GB/s and 64GB capacity at 3.88 pJ/bit [29].

**Area Breakdown.** Fig. 11 shows the area breakdown of the logic die in the 4 GB configuration. PEs dominate the design, occupying 93% of the total area. Within each PE, the tensor compute logic primarily consists of low-bit integer MAC and dequantization units, enabling high area efficiency. Bit-sliced support logic (shifters, multiplexers) introduces negligible overhead, indicating that bit-nested execution can be supported with minimal additional cost. The overall area scales linearly with the number of PEs.

**Table 1: ELMoE-3D system specification.**

Component	Parameter	Value
Logic Die	Technology	ASAP7 7 nm FinFET [8]
	Voltage / Freq.	0.7 V / 1.0 GHz
	Num PEs	{16   32}
	Num MACs / PE	16×32×32
	Throughput (W8A8)	{262   524} TOPS
	Throughput (W4A8)	{524   1048} TOPS
	Aggr. Link	32 GB/s
HB MEM	Streamline Link	128 GB/s
	Num Banks	{16   32}
	Capacity	{4   8} GB
	Bandwidth	{819.2   1638.4} GB/s
EXT MEM	Read Energy	0.43 pJ/bit [45]
	Type	LPDDR5-6400 [29]
	Capacity	64 GB (8 GB/ch)
	Bandwidth	102.4 GB/s
EXT MEM	Read Energy	3.88 pJ/bit [29]

**Table 2: Target MoE models for on-premise deployment.**

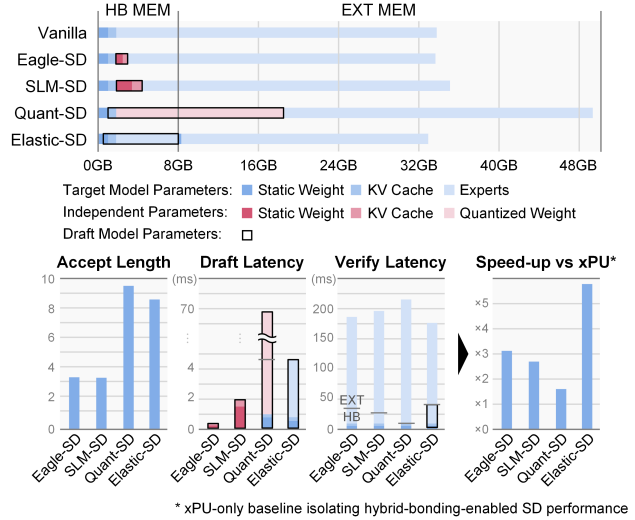
Model	Params		Experts			Notes
	Tot.	Act.	Tot.	Shr.	Top-k.	
Qwen3-30B-A3B	30B	3B	128	-	8	-
GLM-Flash	30B	3B	64	1	4	-
DeepSeek-V2-Lite	15.7B	2.4B	64	2	6	-
GPT-OSS-20B	20B	3.6B	32	-	4	MXFP4 experts

## 7 Evaluation

**Models and Datasets.** Table 2 lists the four target models. Qwen3-30B-A3B [66], GLM-Flash [59], DeepSeek-V2-Lite [10], and GPT-OSS-20B [47] are all ~30B-class MoE models suitable for on-premise deployment, with activated parameters ranging from 2.4B to 3.6B. GPT-OSS-20B provides MXFP4-quantized expert weights, so both Quant-SD and Elastic-SD apply bit-width scaling only to dense layers, with Elastic-SD using expert throttling alone. Datasets include MT-Bench [72] (multi-turn dialogue), GSM8K [9] (math reasoning), Alpaca [58] (instruction following), and HumanEval [4] (code generation). We use 1k sequence length for baseline.

**Inference Framework.** All models use G32 INT8 symmetric quantization with FP16 scaling factors as the baseline precision. Experts are cached in HB under an LRU policy, modeled via power-law LRU approximation [13] calibrated per model and dataset, capturing inter/intra-request routing correlation and batch-size-dependent locality degradation. Speculative decoding uses a tree-based framework [37] with four schemes. *EAGLE-SD* [38] uses an independent lightweight draft head, requiring separate weight storage. *SLM-SD* [15] uses Qwen2.5-1.5B-Instruct [52] as the draft model. *Quant-SD* [60, 61] uses a separately quantized 4-bit copy of the target. *Elastic-SD* (Ours) uses the MSB 4-bit slice of the target weights directly via bit-nested quantization.

**Accelerator Baselines.** We compare against five baseline hardware architectures sharing the same xPU (262–524 TOPS at INT8


**Figure 12: Memory mapping and performance breakdown across SD schemes (Qwen3-30B-A3B, MT-Bench, BS=16, 8GB).**

depending on the HB configuration) and 64 GB LPDDR5 at 102.4 GB/s. *xPU* serves as the baseline, accessing only LPDDR5. *xPU-PIM* adds bank-level analog PIM inside LPDDR5 [18, 19, 29], providing 8× higher internal bandwidth than external memory and 1.64 TOPS of compute throughput. *xPU-LogicPIM* replaces analog PIM with a digital near-memory logic unit [50, 70], providing 4× higher internal bandwidth than external memory and 4× higher compute throughput than *xPU-PIM*. *xPU-NMP* adopts an H2LLM-like architecture [35] by allocating two LPDDR5 channels to NMP, yielding 16 GB capacity, and 13.1 TOPS of compute throughput, scaled to our 7 nm technology. *HB-xPU* bonds the xPU directly onto HB memory with EAGLE-based SD [38]. *Ours* extends HB-xPU with bit-sliced MACs and Elastic-SD.

Latency is evaluated on a cycle-accurate simulator based on Duplex [70], augmented with event-driven modeling for SD scheduling and caching, and integrated with Ramulator [40] for detailed DRAM timing simulation. HB accesses exhibit ~3% lower bandwidth utilization than the roofline due to row-conflict overhead, while external memory achieves within 1% of peak.

### 7.1 SD Scheme Comparison on ELMoE-3D

Fig. 12 (top) illustrates the HB/EXT memory mapping for each SD scheme. Across all schemes, static weights and the KV cache are placed in HB first, while the remaining capacity is allocated to scheme-specific data. *EAGLE-SD* and *SLM-SD* store separate draft model weights and their KV Cache in HB, reducing expert cache space. *Quant-SD* maintains independent 4-bit draft and 8-bit target weight copies across both tiers, representing the worst case as it doubles the per-expert footprint. *Elastic-SD* reuses the target’s MSB 4-bit slice as the draft, requiring no additional draft storage and maximizing residual HB for expert caching.

Fig. 12 (down) shows the breakdown of accept length, draft latency, and verify latency at BS=16. *EAGLE-SD* and *SLM-SD* achieve low draft latency due to their lightweight draft models, but their limited accept length reduces overall efficiency. *Quant-SD* attains

**Table 3: Acceptance rate ( $\alpha$ ) and speedup ( $\Phi_{AR}$ ,  $\Phi_{SD}$ ) across SD schemes on MT-Bench. Bold indicates the best per scenario.**

Target	Draft	batch-size 1			batch-size 4			batch-size 8			batch-size 16		
		$\alpha$	$\Phi_{AR}$	$\Phi_{SD}$	$\alpha$	$\Phi_{AR}$	$\Phi_{SD}$	$\alpha$	$\Phi_{AR}$	$\Phi_{SD}$	$\alpha$	$\Phi_{AR}$	$\Phi_{SD}$
<b>Hybrid-Bonded Memory = 4GB</b>													
Qwen3-30B-A3B [66]	EAGLE3 [38]	0.33	2.83	2.66	0.33	2.24	1.89	0.33	2.06	2.07	0.33	1.83	<b>2.28</b>
	SLM-SD [15]	0.33	2.21	1.70	0.33	1.23	1.53	0.33	1.17	1.76	0.33	1.16	1.96
	Quant-SD [60]	0.95	1.56	1.48	0.95	1.23	1.02	0.95	1.17	1.04	0.95	1.16	1.15
	Elastic-SD	0.66	<b>3.08</b>	2.64	0.57	2.48	<b>2.52</b>	0.48	2.31	<b>2.42</b>	0.36	2.13	2.05
GLM-4.7-Flash [59]	EAGLE3 [38]	0.25	2.50	1.52	0.25	1.83	1.29	0.25	1.60	1.67	0.25	1.55	2.17
	SLM-SD [15]	0.14	1.79	0.60	0.14	1.27	0.74	0.14	1.18	1.00	0.14	1.13	1.27
	Quant-SD [60]	0.83	1.79	0.87	0.83	1.27	0.65	0.83	1.18	0.80	0.83	1.13	1.03
	Elastic-SD	0.61	<b>2.61</b>	2.02	0.55	1.93	<b>2.10</b>	0.50	1.71	<b>2.58</b>	0.47	1.64	<b>3.13</b>
DeepSeek-V2-Lite [10]	EAGLE3 [38]	0.42	2.45	<b>2.63</b>	0.42	1.87	2.80	0.42	1.71	3.65	0.42	1.62	4.21
	SLM-SD [15]	0.38	1.98	1.42	0.38	1.48	1.86	0.38	1.34	2.45	0.38	1.24	2.78
	Quant-SD [60]	0.84	1.65	0.97	0.84	1.22	0.94	0.84	1.15	1.26	0.84	1.12	1.53
	Elastic-SD	0.72	2.51	2.02	0.72	1.92	<b>3.23</b>	0.70	1.82	<b>4.34</b>	0.70	1.72	<b>5.16</b>
GPT-OSS-20B [47]	EAGLE3 [38]	0.23	4.14	2.98	0.23	2.90	1.98	0.23	2.78	2.13	0.23	1.22	2.13
	SLM-SD [15]	0.24	1.81	1.29	0.24	1.33	1.54	0.24	1.25	1.71	0.24	1.22	1.74
	Quant-SD [60]	0.60	5.54	1.65	0.60	4.85	0.74	0.60	4.36	0.69	0.60	3.94	0.74
	Elastic-SD	0.44	<b>5.54</b>	3.08	0.39	<b>4.85</b>	2.86	0.36	<b>4.36</b>	2.78	0.33	<b>3.94</b>	2.56
<b>Hybrid-Bonded Memory = 8GB</b>													
Qwen3-30B-A3B [66]	EAGLE3 [38]	0.33	4.44	4.25	0.33	3.57	2.55	0.33	3.35	2.76	0.33	3.11	3.09
	SLM-SD [15]	0.33	4.11	3.21	0.33	3.22	2.21	0.33	2.94	2.40	0.33	2.77	2.71
	Quant-SD [60]	0.95	1.63	2.15	0.95	1.25	1.44	0.95	1.19	1.42	0.95	1.17	1.56
	Elastic-SD	0.91	<b>4.77</b>	4.58	0.91	3.78	<b>4.71</b>	0.90	3.56	<b>5.29</b>	0.86	3.31	<b>5.78</b>
GLM-4.7-Flash [59]	EAGLE3 [38]	0.25	3.70	2.27	0.25	2.63	1.63	0.25	2.43	2.13	0.25	2.26	2.76
	SLM-SD [15]	0.14	3.34	1.24	0.14	2.36	0.98	0.14	2.09	1.27	0.14	1.93	1.63
	Quant-SD [60]	0.83	1.90	1.30	0.83	1.30	0.90	0.83	1.19	1.08	0.83	1.14	1.38
	Elastic-SD	0.78	<b>3.82</b>	3.10	0.76	2.73	<b>3.31</b>	0.75	2.52	<b>4.39</b>	0.74	2.34	<b>5.74</b>
DeepSeek-V2-Lite [10]	EAGLE3 [38]	0.42	4.22	<b>4.95</b>	0.42	3.08	4.38	0.42	2.90	5.71	0.42	2.74	6.59
	SLM-SD [15]	0.38	3.46	2.87	0.38	2.56	3.01	0.38	2.34	3.86	0.38	2.21	4.40
	Quant-SD [60]	0.84	1.73	1.73	0.84	1.24	2.03	0.84	1.16	2.64	0.84	1.13	3.18
	Elastic-SD	0.84	4.35	3.01	0.83	3.28	<b>4.76</b>	0.83	2.99	<b>6.72</b>	0.82	2.83	<b>8.20</b>
GPT-OSS-20B [47]	EAGLE3 [38]	0.23	10.70	7.13	0.23	9.27	4.36	0.23	9.00	4.27	0.23	8.26	4.08
	SLM-SD [15]	0.24	10.14	4.71	0.24	8.11	3.38	0.24	7.82	3.35	0.24	6.68	3.10
	Quant-SD [60]	0.60	13.95	4.42	0.60	12.24	1.60	0.60	12.03	1.47	0.60	11.05	1.48
	Elastic-SD	0.50	<b>13.95</b>	5.95	0.50	<b>12.24</b>	5.57	0.50	<b>12.03</b>	5.85	0.47	<b>11.05</b>	5.65

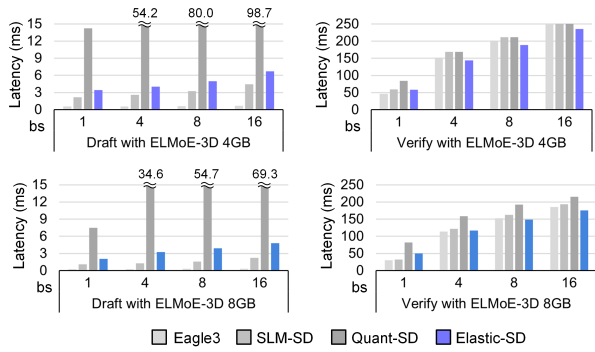
the highest accept length but suffers from large draft and verify costs. In contrast, Elastic-SD maintains high accept length while keeping draft latency low, resulting in a more balanced trade-off between draft and verify costs.

Table 3 reports acceptance rate and speedup across the four schemes on MT-Bench. EAGLE-SD achieves moderate acceptance ( $\alpha=0.23-0.42$ ), but reduced HB cache capacity limits overall speedup and degrades AR latency. SLM-SD shows similar or lower acceptance with limited speedup. Quant-SD attains the highest acceptance ( $\alpha=0.60-0.95$ ), but its speedup remains modest. In contrast, Elastic-SD achieves competitive acceptance ( $\alpha=0.33-0.91$ ) while consistently delivering the highest  $\Phi_{SD}$  and strong  $\Phi_{AR}$  due to larger effective cache capacity.

Elastic-SD gains from two factors. First, no independent draft parameters means larger residual HB for expert caching, improving hit

rates for both AR and verify phases, with the largest gains on models with high expert locality (e.g., GPT-OSS). Second, at large batch sizes, verify cost dominates and draft overhead becomes marginal across all schemes. Speedup then depends on draft-target alignment, where Elastic-SD averages 1.45 $\times$  higher  $\Phi_{SD}$  over EAGLE-SD at  $BS \geq 4$ , reaching up to 2.08 $\times$ . Overall, with Elastic-SD on our architecture, the best-mode speedup over the xPU-only baseline averages 3.4 $\times$  at 4GB and 7.0 $\times$  at 8GB HB capacity.

Fig. 13 shows how the benefit of bit-sliced caching depends on cache capacity and batch size. When HB capacity is limited, bit-sliced caching improves hit rate more than the loss in effective cache size, leading to lower verify latency. As HB capacity increases, this advantage diminishes. At small batch sizes, where cache pressure is low, bit-sliced caching can become less effective, as reflected by the lower verify cost of EAGLE-SD in the 8GB configuration. However,



**Figure 13: Draft and verify latency across batch sizes and HB capacities (Qwen3-30B-A3B, MT-Bench).**

as batch size grows, the active expert set expands and cache capacity becomes the dominant factor, making bit-sliced caching behave similarly to conventional caching without noticeable overhead.

## 7.2 Comparison with Accelerator Baselines

*Speedup.* Fig. 14 reports speedup over the xPU-only baseline across four platforms, four models, four datasets, and batch size 1–16. Dashed lines with triangle markers denote AR mode, and solid lines denote SD mode. Prior memory-centric accelerators show advantages primarily in AR mode at small batch sizes. xPU-PIM performs well for Qwen3 and GLM, while xPU-NMP is strongest for DS2 and GPT-OSS. However, their SD-mode gains are limited, as speculative verification increases compute demand beyond their internal capability. Our design consistently achieves the highest speedup. Elastic-SD improves cache hit rates in both AR and verification, and SD-mode speedup continues to scale with batch size without compute bottleneck. Averaged across all models and datasets at 8GB, our system achieves 6.6× mean speedup over the xPU baseline (up to 12.0×), and 2.2× over the strongest prior baseline (up to 9.9×).

*Energy Consumption.* Fig. 15 reports per-token energy normalized to Ours, decomposed into computation, external memory access, HB memory access, communication, and static power. Blue markers indicate SD-selected configurations. At small batch sizes, PIM, LogicPIM, and NMP process experts locally, but as batch size grows, insufficient internal compute forces offloading to the xPU at high external DRAM energy cost. HB access is 9× more energy-efficient, and our system maximizes HB utilization through Elastic-SD’s caching and weight reuse across both AR and verify phases. Reduced latency further lowers static energy. Overall, Ours reduces energy per token by 4.4× on average (up to 7.2×) compared to the xPU baseline, and 1.4× (up to 4.9×) compared to the best-performing prior accelerator.

## 7.3 Ablation Studies

*A. Expert Locality Analysis.* Fig. 16 characterizes expert access locality along four axes. (a) Cache miss rate rises as batch size increases. It is because batched AR aggregates inter-request expert activations that expand the working set beyond cache coverage. Caching alone cannot sustain low miss rates under batching, motivating SD as a complementary mechanism. (b) For the same token

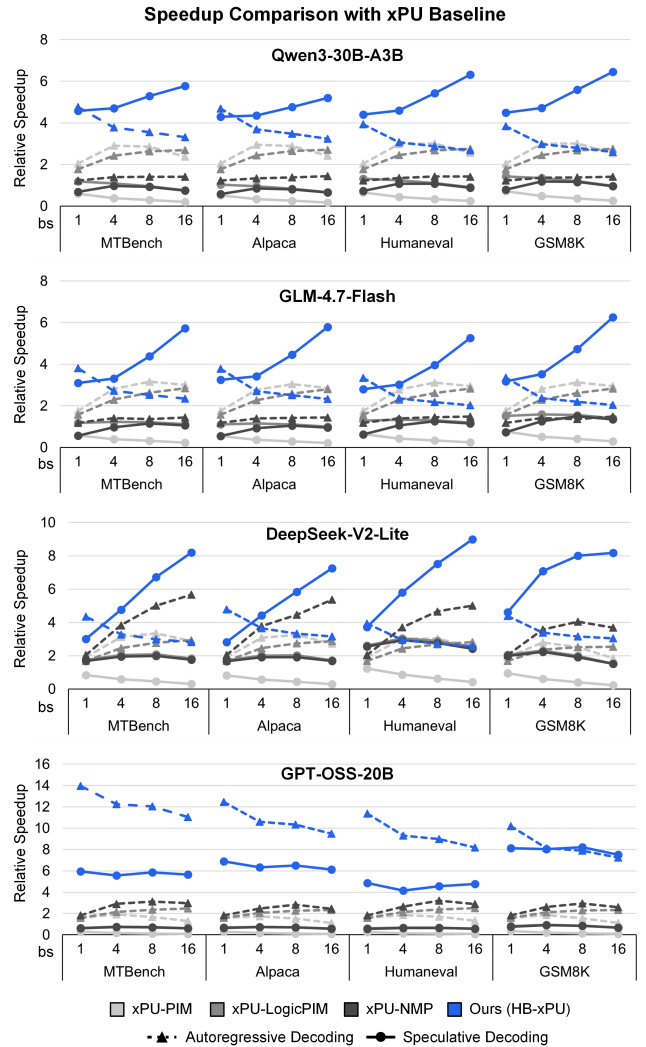


**Figure 14: Speedup over xPU baseline across models and benchmarks (8GB).**

count, intra-request (SD) execution activates far fewer unique experts than inter-request (AR), since draft tokens share context and follow similar routing patterns. This allows a single expert pool to be cached once and reused across multiple draft depths. (c, d) Locality varies substantially across models but modestly across benchmarks, confirming it is primarily a model-level property. Our unified cache-draft design handles both high- and low-locality cases without per-model tuning.

*B. Expert-Axis Elasticity.* Fig. 17(a) compares expert pool selection strategies by acceptance length. Hotness-based selection, which accumulates one-hot routing vectors from preceding draft steps, achieves ~22% higher acceptance than random selection by effectively capturing intra-request routing similarity. Fig. 17(b) compares Elastic SD and Random SD across batch sizes. While Random SD remains unchanged due to its stochastic selection, Elastic SD shows only marginal degradation, thanks to the robustness of the draft model.

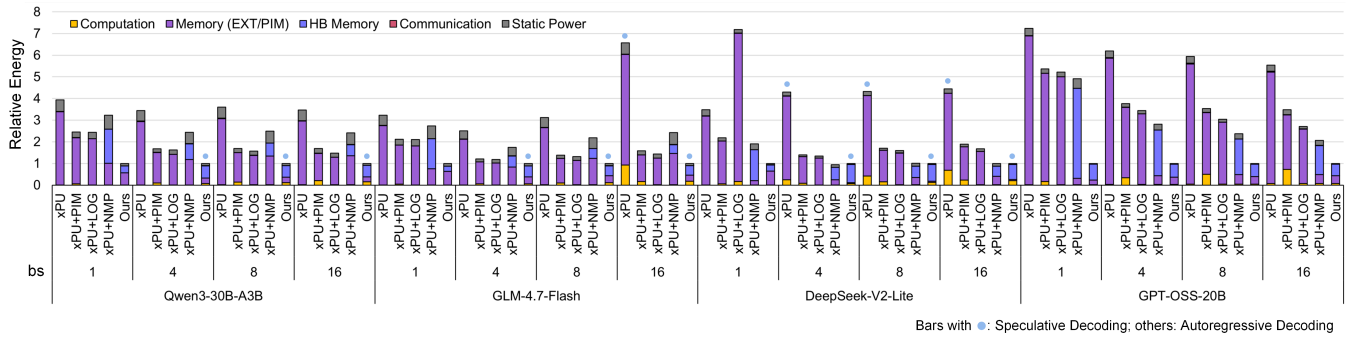


Figure 15: Energy comparison normalized to ours (mJ/token) across models and batch sizes (MT-Bench, 8GB). Blue markers indicate SD-selected configurations.

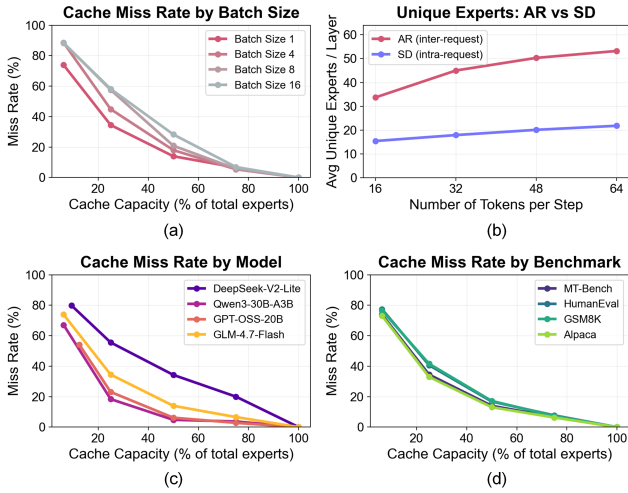


Figure 16: Expert locality analysis (GLM-4.7-Flash, MT-Bench). (a) Miss rate vs. batch size. (b) Unique experts per iteration. (c) Miss rate across models. (d) Miss rate across benchmarks.

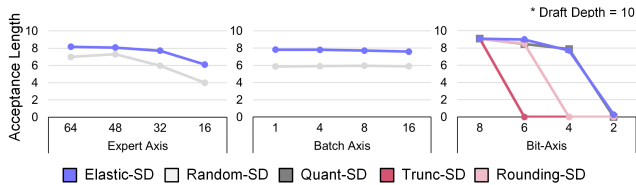


Figure 17: Elasticity analysis (GLM-4.7-Flash, MT-Bench). (a) Expert-axis pool selection. (b) Batch size impact on pool. (c) Bit-axis LSB augmentation effect.

C. *Bit-Axis Elasticity*. Fig. 17(c) compares acceptance rate across MSB-only treatments at varying precisions. LSB augmentation performs comparably to dedicated quantization and consistently outperforms rounding, while simple rounding suffers severe degradation below 4 bits, and truncation fails to function as a draft model. Because LSB augmentation shares the scaling factor with the full 8-bit representation, it occasionally surpasses dedicated quantization, which suffers from independent scale mismatch at low bit-widths.

## 8 Discussion

This work unifies caching and speculative decoding in MoE serving as a single design problem, rather than treating them as separate techniques for different batch regimes. The draft model is interpreted as a cache-resident submodel, enabled by MoE’s intrinsic elasticity along expert and bit axes, while the bit-sliced architecture serves dual purpose as both multi-precision execution and effective cache capacity expansion. This tight coupling between algorithm and architecture is what enables consistent gains across batch sizes within limited HB capacity.

From a system perspective, the primary limitation arises from resource contention within HB capacity. The KV cache is generated deterministically at every layer and must be prioritized for placement in HB. As batch size accumulates and sequence length increases, the KV cache footprint grows rapidly, exerting significant pressure on HB capacity. This reduces the effective space available for expert caching, potentially lowering cache hit rates. As a result, in long-context serving scenarios, the performance benefits of the proposed approach may be diminished.

## 9 Conclusion

In this work, we identify memory activation as the fundamental bottleneck in MoE serving and propose ELMoE-3D, a hybrid-bonding-based HW-SW co-designed framework that unifies caching and speculative decoding. By exploiting the intrinsic elasticity of MoE along both expert and bit axes, we construct Elastic-SD, which serves as both a cache and a self-draft model within limited HB capacity. We further enable native multi-precision support using a bit-sliced datapath without additional hardware overhead, and design an execution engine that effectively utilizes system resources by leveraging the heterogeneous characteristics of memory tiers.

Across diverse models, datasets, and batch sizes, ELMoE-3D with 8GB configuration achieves 6.6× speedup and 4.4× energy reduction over the xPU baseline, and 2.2× speedup and 1.4× energy improvement over prior memory-centric accelerators. These results demonstrate that a unified cache-draft design, coupled with memory-aware execution, is key to efficient on-premise MoE serving.

## References

- [1] Apple Inc. 2026. Apple Mac Studio. <https://www.apple.com/kr/mac-studio/>. Accessed: 2026-04-02.
- [2] Shiyi Cao, Shu Liu, Tyler Griggs, Peter Schafhalter, Xiaoxuan Liu, Ying Sheng, Joseph E. Gonzalez, Matei Zaharia, and Ion Stoica. 2025. MoE-Lightning: High-Throughput MoE Inference on Memory-constrained GPUs. In *Proceedings of the 30th ACM International Conference on Architectural Support for Programming Languages and Operating Systems, Volume 1 (Rotterdam, Netherlands) (ASPLOS '25)*. Association for Computing Machinery, New York, NY, USA, 715–730. <https://doi.org/10.1145/3669940.3707267>
- [3] Liangkun Chen, Zijian Wen, Tian Wu, Xiaoxi Zhang, and Chuan Wu. 2025. SP-MoE: Speculative Decoding and Prefetching for Accelerating MoE-based Model Inference. arXiv:2510.10302 [cs.DC] <https://arxiv.org/abs/2510.10302>
- [4] Mark Chen, Jerry Tworek, Heewoo Jun, Qiming Yuan, Henrique Ponde de Oliveira Pinto, Jared Kaplan, Harri Edwards, Yuri Burda, Nicholas Joseph, Greg Brockman, Alex Ray, Raul Puri, Gretchen Krueger, Michael Petrov, Heidy Khlaaf, Girish Sastry, Pamela Mishkin, Brooke Chan, Scott Gray, Nick Ryder, Mikhail Pavlov, Alethea Power, Lukasz Kaiser, Mohammad Bavarian, Clemens Winter, Philippe Tillet, Felipe Petroski Such, Dave Cummings, Matthias Plappert, Fotios Chantzis, Elizabeth Barnes, Ariel Herbert-Voss, William Hebgen Guss, Alex Nichol, Alex Paino, Nikolas Tezak, Jie Tang, Igor Babuschkin, Suchir Balaji, Shantanu Jain, William Saunders, Christopher Hesse, Andrew N. Carr, Jan Leike, Josh Achiam, Vedant Misra, Evan Morikawa, Alec Radford, Matthew Knight, Miles Brundage, Mira Murati, Katie Mayer, Peter Welinder, Bob McGrew, Dario Amodei, Sam McCandlish, Ilya Sutskever, and Wojciech Zaremba. 2021. Evaluating Large Language Models Trained on Code. arXiv:2107.03374 [cs.LG] <https://arxiv.org/abs/2107.03374>
- [5] Insu Choi, Young-Seo Yoon, and Joon-Sung Yang. 2025. Bit-slice Architecture for DNN Acceleration with Slice-level Sparsity Enhancement and Exploitation. In *2025 IEEE International Symposium on High Performance Computer Architecture (HPCA)*. 821–835. <https://doi.org/10.1109/HPCA61900.2025.00067>
- [6] Yuseon Choi, Sangjin Kim, Jungjun Oh, Byeongcheol Kim, and Hoi-Jun Yoo. 2026. SeVeDo: A Heterogeneous Transformer Accelerator for Low-Bit Inference via Hierarchical Group Quantization and SVD-Guided Mixed Precision. arXiv:2512.12930 [cs.LG] <https://arxiv.org/abs/2512.12930>
- [7] Yuseon Choi, Sangjin Kim, Jungjun Oh, Gwangtae Park, Byeongcheol Kim, and Hoi-Jun Yoo. 2026. SliceMoE: Bit-Sliced Expert Caching under Miss-Rate Constraints for Efficient MoE Inference. arXiv:2512.12990 [cs.AR] <https://arxiv.org/abs/2512.12990>
- [8] Lawrence T. Clark, Vinay Vashishtha, Lucian Shifren, Aditya Gujja, Saurabh Sinha, Brian Cline, Chandarasekaran Ramamurthy, and Greg Yeric. 2016. ASAP7: A 7-nm finFET predictive process design kit. *Microelectronics Journal* 53 (2016), 105–115. <https://doi.org/10.1016/j.mejo.2016.04.006>
- [9] Karl Cobbe, Vineet Kosaraju, Mohammad Bavarian, Mark Chen, Heewoo Jun, Lukasz Kaiser, Matthias Plappert, Jerry Tworek, Jacob Hilton, Reiichiro Nakano, Christopher Hesse, and John Schulman. 2021. Training Verifiers to Solve Math Word Problems. arXiv:2110.14168 [cs.LG] <https://arxiv.org/abs/2110.14168>
- [10] DeepSeek-AI, Aixin Liu, Bei Feng, Bin Wang, Bingxuan Wang, Bo Liu, Chenggang Zhao, Chengqi Deng, Chong Ruan, Damai Dai, Daya Guo, Dejian Yang, Deli Chen, Dongjie Ji, Erhang Li, Fangyun Lin, Fuli Luo, Guangbo Hao, Guanting Chen, Guowei Li, H. Zhang, Hanwei Xu, Hao Yang, Haowei Zhang, Honghui Ding, Huajian Xin, Huazuo Gao, Hui Li, Hui Qu, J. L. Cai, Jian Liang, Jianzhong Guo, Jiaqi Ni, Jiashi Li, Jin Chen, Jingyang Yuan, Junjie Qiu, Junxiao Song, Kai Dong, Kaige Gao, Kang Guan, Lean Wang, Lecong Zhang, Lei Xu, Leyi Xia, Liang Zhao, Liyue Zhang, Meng Li, Miaojun Wang, Mingchuan Zhang, Minghua Zhang, Minghui Tang, Mingming Li, Ning Tian, Panpan Huang, Peiyi Wang, Peng Zhang, Qihao Zhu, Qinyu Chen, Qiushi Du, R. J. Chen, R. L. Jin, Ruiqi Ge, Ruizhe Pan, Runxin Xu, Ruyi Chen, S. S. Li, Shanghao Lu, Shangan Zhou, Shanhuang Chen, Shaoqing Wu, Shengfeng Ye, Shirong Ma, Shiyu Wang, Shuang Zhou, Shuiping Yu, Shunfeng Zhou, Size Zheng, T. Wang, Tian Pei, Tian Yuan, Tianyu Sun, W. L. Xiao, Wangding Zeng, Wei An, Wen Liu, Wenfeng Liang, Wenjun Gao, Wentao Zhang, X. Q. Li, Xiangyue Jin, Xianzu Wang, Xiao Bi, Xiaodong Liu, Xiaohan Wang, Xiaojin Shen, Xiaokang Chen, Xiaosha Chen, Xiaotao Nie, Xiaowen Sun, Xiaoxiang Wang, Xin Liu, Xin Xie, Xingkai Yu, Xinnan Song, Xinyi Zhou, Xinyu Yang, Xuan Lu, Xuecheng Su, Y. Wu, Y. K. Li, Y. X. Wei, Y. X. Zhu, Yanhong Xu, Yanping Huang, Yao Li, Yao Zhao, Yaofeng Sun, Yaohui Li, Yaohui Wang, Yi Zheng, Yichao Zhang, Yiliang Xiong, Yulong Zhao, Ying He, Ying Tang, Yishi Piao, Yixin Dong, Yixuan Tan, Yiyuan Liu, Yongji Wang, Yongqiang Guo, Yuchen Zhu, Yudian Wang, Yuheng Zou, Yukun Zha, Yunxian Ma, Yuting Yan, Yuxiang You, Yuxuan Liu, Z. Z. Ren, Zehui Ren, Zhangli Sha, Zhe Fu, Zhen Huang, Zhen Zhang, Zhenda Xie, Zhewen Hao, Zhihong Shao, Zhiyuan Wen, Zhipeng Xu, Zhongyuan Zhang, Zhuoshu Li, Zihan Wang, Zihui Gu, Zilin Li, and Ziwei Xie. 2024. DeepSeek-V2: A Strong, Economical, and Efficient Mixture-of-Experts Language Model. arXiv:2405.04434 [cs.CL] <https://arxiv.org/abs/2405.04434>
- [11] Pingcheng Dong, Yonghao Tan, Xuejiao Liu, Peng Luo, Yu Liu, Di Pang, Songchen Ma, Xijie Huang, Shih-Yang Liu, Dong Zhang, Zhichao Lu, Luhong Liang, Chi-Ying Tsui, Fengbin Tu, Liang Zhao, and Kwang-Zing Cheng. 2026. 31.1 A 14.08-to-135.69Token/s ReRAM-on-Logic Stacked Outlier-Free Large-Language-Model Accelerator with Block-Clustered Weight-Compression and Adaptive Parallel-Speculative-Decoding. In *2026 IEEE International Solid-State Circuits Conference (ISSCC)*, Vol. 69. 532–534. <https://doi.org/10.1109/ISSCC49663.2026.11409211>
- [12] Mostafa Elhoushi, Akshat Shrivastava, Diana Liskovich, Basil Hosmer, Bram Wasti, Liangzhen Lai, Anas Mahmoud, Bilge Acun, Saurabh Agarwal, Ahmed Roman, Ahmed Aly, Beidi Chen, and Carole-Jean Wu. 2024. LayerSkip: Enabling Early Exit Inference and Self-Speculative Decoding. In *Proceedings of the 62nd Annual Meeting of the Association for Computational Linguistics (Volume 1: Long Papers)*, Lun-Wei Ku, Andre Martins, and Vivek Srikumar (Eds.). Association for Computational Linguistics, Bangkok, Thailand, 12622–12642. <https://doi.org/10.18653/v1/2024.acl-long.681>
- [13] Christine Fricker, Philippe Robert, and James Roberts. 2012. A versatile and accurate approximation for LRU cache performance. arXiv:1202.3974 [cs.NI] <https://arxiv.org/abs/1202.3974>
- [14] Evangelos Georganas, Dhiraj Kalamkar, Alexander Kozlov, and Alexander Heinecke. 2025. ML-SpecQD: Multi-Level Speculative Decoding with Quantized Drafts. arXiv:2503.13565 [cs.CL] <https://arxiv.org/abs/2503.13565>
- [15] Raghav Goel, Mukul Gagrani, Wonseok Jeon, Junyoung Park, Mingyu Lee, and Christopher Lott. 2024. Direct Alignment of Draft Model for Speculative Decoding with Chat-Fine-tuned LLMs. In *ICLR 2024 Workshop on Mathematical and Empirical Understanding of Foundation Models*. <https://openreview.net/forum?id=126PpV2CoO>
- [16] Sangwoo Ha, Jingu Lee, Youngjin Moon, Sunjoo Whang, Wooyoung Jo, Gwangtae Park, Sangjin Kim, Soyeon Um, Junha Ryu, Yurim Jo, and Hoi-Jun Yoo. 2026. SMO-LPU: 122.1μJ/Token Sparse MoE-Based Speculative Decoding Language Processing Unit with Adaptive-Ofload NPU-CIM Core. In *2026 IEEE International Solid-State Circuits Conference (ISSCC)*, Vol. 69. 312–314. <https://doi.org/10.1109/ISSCC49663.2026.11409285>
- [17] Sanghyeok Han, Byungkuk Yoon, Gyeonghwan Park, Choungki Song, Dongkyun Kim, and Jae-Joon Kim. 2025. Near-Memory LLM Inference Processor based on 3D DRAM-to-Logic Hybrid Bonding. In *Proceedings of the 62nd Annual ACM/IEEE Design Automation Conference (San Francisco, California, United States) (DAC '25)*. IEEE Press, Article 205, 7 pages. <https://doi.org/10.1109/DAC63849.2025.11132870>
- [18] Siyuan He, Zhantong Zhu, Yandong He, and Tianyu Jia. 2025. LP-Spec: Leveraging LPDDR PIM for Efficient LLM Mobile Speculative Inference with Architecture-Dataflow Co-Optimization. , 9 pages. <https://doi.org/10.1109/ICCAD66269.2025.11240889>
- [19] Guseul Heo, Sangyeop Lee, Jaehong Cho, Hyunmin Choi, Sanghyeon Lee, Hyungkyu Ham, Gwangsun Kim, Divya Mahajan, and Jongse Park. 2024. Neupims: Npu-pim heterogeneous acceleration for batched llm inferencing. In *Proceedings of the 29th ACM International Conference on Architectural Support for Programming Languages and Operating Systems, Volume 3*. 722–737.
- [20] Hanbo Huang, Yihan Li, Bowen Jiang, Lin Liu, Bo Jiang, Ruoyun Sun, Zhuotao Liu, and Shiyu Liang. 2025. On-Premises LLM Deployment Demands a Middle Path: Preserving Privacy Without Sacrificing Model Confidentiality. In *ICLR 2025 Workshop on Building Trust in Language Models and Applications*. <https://openreview.net/forum?id=u61yT9ZKEZ>
- [21] Zongle Huang, Lei Zhu, ZongYuan Zhan, Ting Hu, Weikai Mao, Xianzhi Yu, Yongpan Liu, and Tianyu Zhang. 2025. MoESD: Unveil Speculative Decoding's Potential for Accelerating Sparse MoE. In *The Thirty-ninth Annual Conference on Neural Information Processing Systems*. <https://openreview.net/forum?id=FAeU7516MR>
- [22] Raymond Hung, Gilbert See, Ying Wang, Chang Bum Yong, Ke Zheng, Yauloong Chang, Avi Shantaram, Ruiping Wang, Arvind Sundararajan, Jonathan Abdilla, Nithyananda Hegde, Stefan Schmid, Djuro Bikaljevic, and Manfred Glantschnig. 2024. Enabling Die-to-Wafer Hybrid Bonding for the Next Generation Advanced 3D Packaging. In *2024 IEEE 74th Electronic Components and Technology Conference (ECTC)*. 778–783. <https://doi.org/10.1109/ECTC51529.2024.00127>
- [23] Rangi Hwang, Jianyu Wei, Shijie Cao, Changho Hwang, Xiaohu Tang, Ting Cao, and Mao Yang. 2025. Pre-Gated MoE: An Algorithm-System Co-Design for Fast and Scalable Mixture-of-Expert Inference. In *Proceedings of the 51st Annual International Symposium on Computer Architecture (Buenos Aires, Argentina) (ISCA '24)*. IEEE Press, 1018–1031. <https://doi.org/10.1109/ISCA59077.2024.00078>
- [24] Dongseok Im, Gwangtae Park, Zhiyong Li, Junha Ryu, and Hoi-Jun Yoo. 2023. Sibia: Signed Bit-slice Architecture for Dense DNN Acceleration with Slice-level Sparsity Exploitation. In *2023 IEEE International Symposium on High-Performance Computer Architecture (HPCA)*. 69–80. <https://doi.org/10.1109/HPCA56546.2023.10071031>
- [25] JEDEC Solid State Technology Association. 2019. JESD209-5: Low Power Double Data Rate 5 (LPDDR5). <https://www.jedec.org/standards-documents/docs/jesd209-5>. Standard specification.

- [26] Dongyun Kam, Myeongji Yun, Sunwoo Yoo, Seungwoo Hong, Zhengya Zhang, and Youngjo Lee. 2025. Panacea: Novel DNN Accelerator using Accuracy-Preserving Asymmetric Quantization and Energy-Saving Bit-Slice Sparsity. In *2025 IEEE International Symposium on High Performance Computer Architecture (HPCA)*. IEEE Computer Society, Los Alamitos, CA, USA, 701–715. <https://doi.org/10.1109/HPCA61900.2025.00059>
- [27] Jared Kaplan, Sam McCandlish, Tom Henighan, Tom B. Brown, Benjamin Chess, Rewon Child, Scott Gray, Alec Radford, Jeffrey Wu, and Dario Amodei. 2020. Scaling Laws for Neural Language Models. arXiv:2001.08361 [cs.LG] <https://arxiv.org/abs/2001.08361>
- [28] Jinhee Kim, Seoyeon Yoon, Taeho Lee, Joo Chan Lee, Kang Eun Jeon, and Jong Hwan Ko. 2025. TruncQuant: Truncation-Ready Quantization for DNNs with Flexible Weight Bit Precision. arXiv:2506.11431 [cs.LG] <https://arxiv.org/abs/2506.11431>
- [29] Jin Hyun Kim, Yuhwan Ro, Jinin So, Sukhan Lee, Shin-haeng Kang, YeonGon Cho, Hyeonsu Kim, Byeongho Kim, Kyungsoo Kim, Sangsoo Park, Jin-Seong Kim, Sanghoon Cha, Won-Jo Lee, Jin Jung, Jong-Geon Lee, Jieun Lee, JoonHo Song, Seungwon Lee, Jeonghyeon Cho, Jaehoon Yu, and Kyomin Sohn. 2023. Samsung PIM/PNM for Transformer Based AI : Energy Efficiency on PIM/PNM Cluster. In *2023 IEEE Hot Chips 35 Symposium (HCS)*, 1–31. <https://doi.org/10.1109/HCS59251.2023.10254711>
- [30] Sangjin Kim, Jungjun Oh, Byeongcheol Kim, Yuseon Choi, Gwangtae Park, and Hoi-Jun Yoo. 2026. 31.2 Revolver: Low-Bit GenAI Accelerator for Distilled-Model and CoT with Phase-Aware-Quantization and Rotation-Based Integer-Scaled Group Quantization. In *2026 IEEE International Solid-State Circuits Conference (ISSCC)*, Vol. 69, 534–536. <https://doi.org/10.1109/ISSCC49663.2026.11409015>
- [31] Maximilian Kleinegger, Elvir Crncević, and Dan Alistarh. 2026. Mat-GPTQ: Accurate and Efficient Post-Training Matryoshka Quantization. arXiv:2602.03537 [cs.LG] <https://arxiv.org/abs/2602.03537>
- [32] Phil C. Knag, Gregory K. Chen, Shanshan Xie, Satish Yada, Wei Wu, Yu-Shiang Lin, Alexander Kashirin, Xiemei Meng, Russell Criss, Ana Sonia Leon, Carlos Tokunaga, Ram K. Krishnamurthy, and James W. Tschanz. 2026. 10.6 A Hybrid-Bonded 12.1Tops/mm<sup>2</sup> 5-6-Core DNN Processor with 2.5Tb/s/mm<sup>2</sup> 3D Network on Chip. In *2026 IEEE International Solid-State Circuits Conference (ISSCC)*, Vol. 69, 178–180. <https://doi.org/10.1109/ISSCC49663.2026.11409347>
- [33] Juhyoung Lee, Dongjoo Shin, Jinsu Lee, Jinmook Lee, Sanghoon Kang, and Hoi-Jun Yoo. 2019. A Full HD 60 fps CNN Super Resolution Processor with Selective Caching based Layer Fusion for Mobile Devices. In *2019 Symposium on VLSI Circuits*. C302–C303. <https://doi.org/10.1109/ISSCC49663.2026.11409347>
- [34] Yaniv Leviathan, Matan Kalman, and Yossi Matias. 2023. Fast inference from transformers via speculative decoding. In *Proceedings of the 40th International Conference on Machine Learning (Honolulu, Hawaii, USA) (ICML '23)*. JMLR.org, Article 795, 13 pages.
- [35] Cong Li, Yihan Yin, Xintong Wu, Jingchen Zhu, Zhutianya Gao, Dimin Niu, Qiang Wu, Xin Si, Yuan Xie, Chen Zhang, and Guangyu Sun. 2025. H2-LLM: Hardware-Dataflow Co-Exploration for Heterogeneous Hybrid-Bonding-based Low-Batch LLM Inference. In *Proceedings of the 52nd Annual International Symposium on Computer Architecture (ISCA '25)*. Association for Computing Machinery, New York, NY, USA, 194–210. <https://doi.org/10.1145/3695053.3731008>
- [36] Yuhui Li, Fangyun Wei, Chao Zhang, and Hongyang Zhang. 2024. EAGLE-2: Faster Inference of Language Models with Dynamic Draft Trees. In *Proceedings of the 2024 Conference on Empirical Methods in Natural Language Processing*, Yaser Al-Onaizan, Mohit Bansal, and Yun-Nung Chen (Eds.). Association for Computational Linguistics, Miami, Florida, USA, 7421–7432. <https://doi.org/10.18653/v1/2024.emnlp-main.422>
- [37] Yuhui Li, Fangyun Wei, Chao Zhang, and Hongyang Zhang. 2024. EAGLE: speculative sampling requires rethinking feature uncertainty. In *Proceedings of the 41st International Conference on Machine Learning (Vienna, Austria) (ICML '24)*. JMLR.org, Article 1162, 14 pages.
- [38] Yuhui Li, Fangyun Wei, Chao Zhang, and Hongyang Zhang. 2025. EAGLE-3: Scaling up Inference Acceleration of Large Language Models via Training-Time Test. arXiv:2503.01840 [cs.CL] <https://arxiv.org/abs/2503.01840>
- [39] Jiahao Liu, Qifan Wang, Jingang Wang, and Xunliang Cai. 2024. Speculative Decoding via Early-exiting for Faster LLM Inference with Thompson Sampling Control Mechanism. In *Findings of the Association for Computational Linguistics: ACL 2024*, Lun-Wei Ku, Andre Martins, and Vivek Srikumar (Eds.). Association for Computational Linguistics, Bangkok, Thailand, 3027–3043. <https://doi.org/10.18653/v1/2024.findings-acl.179>
- [40] Haocong Luo, Yahya Can Tuğrul, F. Nisa Bostancı, Ataberk Olgun, A. Giray Yağlıkçı, and Onur Mutlu. 2024. Ramulator 2.0: A Modern, Modular, and Extensible DRAM Simulator. *IEEE Computer Architecture Letters* 23, 1 (2024), 112–116. <https://doi.org/10.1109/LCA.2023.3333759>
- [41] Bradley McDanel, Steven Li, Sruthikesh Surineni, and Harshit Khaitan. 2026. MoE-Spec: Expert Budgeting for Efficient Speculative Decoding. arXiv:2602.16052 [cs.LG] <https://arxiv.org/abs/2602.16052>
- [42] Micron Technology, Inc. 2023. LPDDR5/LPDDR5X SDRAM Datasheet. <https://www.micron.com/>. Technical documentation.
- [43] Seungjae Moon, Jung-Hoon Kim, Junsoo Kim, Seongmin Hong, Junseo Cha, Minsu Kim, Sukbin Lim, Gyubin Choi, Dongjin Seo, Jongho Kim, Hunjong Lee, Hyunjun Park, Ryeowook Ko, Soongyu Choi, Jongse Park, Jinwon Lee, and Joo-Young Kim. 2024. A Latency Processing Unit: A Latency-Optimized and Highly Scalable Processor for Large Language Model Inference. *IEEE Micro* 44, 6 (2024), 17–33. <https://doi.org/10.1109/MM.2024.3420728>
- [44] Pranav Ajit Nair, Puranjay Datta, Jeff Dean, Prateek Jain, and Aditya Kusupati. 2025. Matryoshka Quantization. In *Forty-second International Conference on Machine Learning*. <https://openreview.net/forum?id=phVWcUSGYP>
- [45] Dimin Niu, Shuangchen Li, Yuhao Wang, Wei Han, Zhe Zhang, Yijin Guan, Tianchan Guan, Fei Sun, Fei Xue, Lide Duan, Yuanwei Fang, Hongzhong Zheng, Xiping Jiang, Song Wang, Fengguo Zuo, Yubing Yang, Bing Yu, Qiwei Ren, and Yuan Xie. 2022. 184QPS/W 64Mb/mm<sup>2</sup>3D Logic-to-DRAM Hybrid Bonding with Process-Near-Memory Engine for Recommendation System. In *2022 IEEE International Solid-State Circuits Conference (ISSCC)*, Vol. 65, 1–3. <https://doi.org/10.1109/ISSCC42614.2022.9731694>
- [46] NVIDIA. 2026. NVIDIA DGX Spark. <https://www.nvidia.com/ko-kr/products/workstations/dgx-spark/>. Accessed: 2026-04-02.
- [47] OpenAI, Sandhini Agarwal, Lama Ahmad, Jason Ai, Sam Altman, Andy Applebaum, Edwin Arbus, Rahul K. Arora, Yu Bai, Bowen Baker, Haiming Bao, Boaz Barak, Ally Bennett, Tyler Bertao, Nivedita Brett, Eugene Brevdo, Greg Brockman, Sebastien Bubeck, Che Chang, Kai Chen, Mark Chen, Enoch Cheung, Aidan Clark, Dan Cook, Marat Dukhan, Casey Dvorkan, Kevin Fries, Vlad Fomenko, Timur Garipov, Kristian Georgiev, Mia Glaese, Tarun Gogineni, Adam Goucher, Lukas Gross, Katia Gil Guzman, John Hallman, Jackie Hehir, Johannes Heidecke, Alec Helyar, Haitang Hu, Romain Huet, Jacob Huh, Saachi Jain, Zach Johnson, Chris Koch, Irina Kofman, Dominik Kundel, Jason Kwon, Volodymyr Knyrylov, Elaine Ya Le, Guillaume Leclerc, James Park Lennon, Scott Lessans, Mario Lezcano-Casado, Yuanzhi Li, Zhuohan Li, Ji Lin, Jordan Liss, Lily, Liu, Jiancheng Liu, Kevin Lu, Chuan Lu, Zoran Martinovic, Lindsay McCallum, Josh McGrath, Scott McKinney, Aidan McLaughlin, Song Mei, Steve Mostovoy, Tong Mu, Gideon Myles, Alexander Neitz, Alex Nichol, Jakub Pachocki, Alex Paino, Dana Palmie, Ashley Pantuliano, Giambattista Parascandolo, Jongsoo Park, Leher Pathak, Carolina Paz, Ludovic Peran, Dmitry Pimenov, Michelle Pokrass, Elizabeth Proehl, Huida Qiu, Gaby Rila, Filippo Raso, Hongyu Ren, Kimmy Richardson, David Robinson, Bob Rotsted, Hadi Salman, Suvansh Sanjeev, Max Schwarzer, D. Sculley, Harshit Sikchi, Kendal Simon, Karan Singhal, Yang Song, Dane Stuckey, Zhiqing Sun, Philippe Tillet, Sam Toizer, Foivos Tsimpouras, Nikhil Vyas, Eric Wallace, Xin Wang, Miles Wang, Olivia Watkins, Kevin Weir, Amy Wendling, Kevin Whinnery, Cedric Whitney, Hannah Wong, Lin Yang, Yu Yang, Michihiro Yasunaga, Kristen Ying, Wojciech Zaremba, Wenting Zhang, Cyril Zhang, Brian Zhang, Eddie Zhang, and Shengjia Zhao. 2025. gpt-oss-120b & gpt-oss-20b Model Card. arXiv:2508.10925 [cs.CL] <https://arxiv.org/abs/2508.10925>
- [48] Yue Pan, Zihan Xia, Po-Kai Hsu, Lanxiang Hu, Hyungyu Kim, Janak Sharda, Minxuan Zhou, Nam Sung Kim, Shimeng Yu, Tianjia Rosing, and Mingu Kang. 2025. Stratum: System-Hardware Co-Design with Tiered Monolithic 3D-Stackable DRAM for Efficient MoE Serving. In *Proceedings of the 58th IEEE/ACM International Symposium on Microarchitecture (MICRO '25)*. Association for Computing Machinery, New York, NY, USA, 1–17. <https://doi.org/10.1145/3725843.3756043>
- [49] Gunho Park, Jeongin Bae, Beomseok Kwon, Byeongwook Kim, Se Jung Kwon, and Dongsoo Lee. 2026. AnyBCQ: Hardware Efficient Flexible Binary-Coded Quantization for Multi-Precision LLMs. In *The Fourteenth International Conference on Learning Representations*. <https://openreview.net/forum?id=XPIEkFdEDi>
- [50] Jaehyun Park, Jaewan Choi, Kwanhee Kyung, Michael Jaemin Kim, Yongsuk Kwon, Nam Sung Kim, and Jung Ho Ahn. 2024. AttAcc! Unleashing the Power of PIM for Batched Transformer-based Generative Model Inference. In *Proceedings of the 29th ACM International Conference on Architectural Support for Programming Languages and Operating Systems, Volume 2 (La Jolla, CA, USA) (ASPLOS '24)*. Association for Computing Machinery, New York, NY, USA, 103–119. <https://doi.org/10.1145/3620665.3640422>
- [51] Yeonhong Park, Jake Hyun, SangLyu Cho, Bonggeun Sim, and Jae W. Lee. 2024. Any-precision LLM: low-cost deployment of multiple, different-sized LLMs. In *Proceedings of the 41st International Conference on Machine Learning (Vienna, Austria) (ICML '24)*. JMLR.org, Article 1607, 20 pages.
- [52] Qwen, An Yang, Baosong Yang, Beichen Zhang, Binuyan Hui, Bo Zheng, Bowen Yu, Chengyuan Li, Dayiheng Liu, Fei Huang, Haoran Wei, Huan Lin, Jian Yang, Jianhong Tu, Jianwei Zhang, Jianxin Yang, Jiayi Yang, Jingren Zhou, Junyang Lin, Kai Dang, Keming Lu, Keqin Bao, Kexin Yang, Le Yu, Mei Li, Mingfeng Xue, Pei Zhu, Qin Zhu, Rui Men, Runji Tan, Tianhao Li, Tianyi Tang, Tingyu Xia, Xingzhang Ren, Xuancheng Ren, Yang Fan, Yang Su, Yichang Zhang, Yu Wan, Yuyang Liu, Zeyu Cui, Zhenru Zhang, and Zihan Qiu. 2025. Qwen2.5 Technical Report. arXiv:2412.15115 [cs.CL] <https://arxiv.org/abs/2412.15115>
- [53] Semyon Savkin, Eitan Porat, Or Ordentlich, and Yury Polyanskiy. 2025. NestQuant: nested lattice quantization for matrix products and LLMs. In *Forty-second International Conference on Machine Learning*. <https://openreview.net/forum?id=4OWGON33HE>
- [54] Anish Saxena, Po-An Tsai, Hritvik Taneja, Aamer Jaleel, and Moinuddin Qureshi. 2025. Utility-Driven Speculative Decoding for Mixture-of-Experts.

- arXiv:2506.20675 [cs.DC] <https://arxiv.org/abs/2506.20675>
- [55] Hardik Sharma, Jongse Park, Naveen Suda, Liangzhen Lai, Benson Chau, Joon Kyung Kim, Vikas Chandra, and Hadi Esmaeilzadeh. 2018. Bit fusion: bit-level dynamically composable architecture for accelerating deep neural networks. In *Proceedings of the 45th Annual International Symposium on Computer Architecture* (Los Angeles, California) (ISCA '18). IEEE Press, 764–775. <https://doi.org/10.1109/ISCA.2018.00069>
- [56] Noam Shazeer, Azalia Mirhoseini, Krzysztof Maziarz, Andy Davis, Quoc V. Le, Geoffrey E. Hinton, and Jeff Dean. 2017. Outrageously Large Neural Networks: The Sparsely-Gated Mixture-of-Experts Layer. In *5th International Conference on Learning Representations, ICLR 2017, Toulon, France, April 24–26, 2017, Conference Track Proceedings*. OpenReview.net. <https://openreview.net/forum?id=B1ckMDqlg>
- [57] Andrii Skliar, Ties van Rozendaal, Romain Lepert, Todor Boinovski, Mart Van Baalen, Markus Nagel, Paul N. Whatmough, and Babak Ehteshami Bejnordi. 2025. Mixture of Cache-Conditional Experts for Efficient Mobile Device Inference. *Transactions on Machine Learning Research* (2025). <https://openreview.net/forum?id=ul4W26kEKz>
- [58] Rohan Taori, Ishaan Gulrajani, Tianyi Zhang, Yann Dubois, and Xuechen Li. 2023. Alpaca: A Strong, Replicable Instruction-Following Model. <https://crfm.stanford.edu/2023/03/13/alpaca.html>. Stanford Center for Research on Foundation Models (CRFM).
- [59] 5 Team, Aohan Zeng, Xin Lv, Qinkai Zheng, Zhenyu Hou, Bin Chen, Chengxing Xie, Cunxiang Wang, Da Yin, Hao Zeng, Jiajie Zhang, Kedong Wang, Lucent Zhong, Mingdao Liu, Rui Lu, Shulin Cao, Xiaohan Zhang, Xuancheng Huang, Yao Wei, Yean Cheng, Yifan An, Yilin Niu, Yuanhao Wen, Yushi Bai, Zhengxiao Du, Zihan Wang, Zilin Zhu, Bohan Zhang, Bosi Wen, Bowen Wu, Bowen Xu, Can Huang, Casey Zhao, Changpeng Cai, Chao Yu, Chen Li, Chendi Ge, Chenghua Huang, Chenhui Zhang, Chenxi Xu, Chenzheng Zhu, Chuang Li, Congfeng Yin, Daoyan Lin, Dayong Yang, Dazhi Jiang, Ding Ai, Erle Zhu, Fei Wang, Gengzheng Pan, Guo Wang, Hailong Sun, Haitao Li, Haiyang Li, Haiyi Hu, Hanyu Zhang, Hao Peng, Hao Tai, Haoke Zhang, Haoran Wang, Haoyu Yang, He Liu, He Zhao, Hongwei Liu, Hongxi Yan, Huan Liu, Huilong Chen, Ji Li, Jiajing Zhao, Jiamin Ren, Jian Jiao, Jiani Zhao, Jianyang Yan, Jiaqi Wang, Jiayi Gui, Jiayue Zhao, Jie Liu, Jijie Li, Jing Li, Jing Lu, Jingsen Wang, Jingwei Yuan, Jingxuan Li, Jingzhao Du, Jinhua Du, Jinxin Liu, Junkai Zhi, Junli Gao, Ke Wang, Lekang Yang, Liang Xu, Lin Fan, Lindong Wu, Lintao Ding, Lu Wang, Man Zhang, Minghao Li, Minghuan Xu, Mingming Zhao, Mingshu Zhai, Pengfan Du, Qian Dong, Shangde Lei, Shangqing Tu, Shangtong Yang, Shaoyou Lu, Shijie Li, Shuang Li, Shuang-Li, Shuxun Yang, Sibo Yi, Tianshu Yu, Wei Tian, Weihang Wang, Wenbo Yu, Weng Lam Tam, Wenjie Liang, Wentao Liu, Xiao Wang, Xiaohan Jia, Xiaotao Gu, Xiaoying Ling, Xin Wang, Xing Fan, Xingru Pan, Xinyuan Zhang, Xinze Zhang, Xiuqing Fu, Xunkai Zhang, Yabo Xu, Yandong Wu, Yida Lu, Yidong Wang, Yilin Zhou, Yiming Pan, Ying Zhang, Yingli Wang, Yingru Li, Yinpei Su, Yipeng Geng, Yitong Zhu, Yongkun Yang, Yuhang Li, Yuhao Wu, Yujiang Li, Yunan Liu, Yunqing Wang, Yuntao Li, Yuxuan Zhang, Zezhen Liu, Zhen Yang, Zhengda Zhou, Zhongpei Qiao, Zhuoer Feng, Zhuorui Liu, Zichen Zhang, Zihan Wang, Zijun Yao, Zikang Wang, Ziqiang Liu, Ziwei Chai, Zixuan Li, Zuodong Zhao, Wenguang Chen, Jidong Zhai, Bin Xu, Minlie Huang, Hongning Wang, Juanzi Li, Yuxiao Dong, and Jie Tang. 2025. GLM-4.5: Agentic, Reasoning, and Coding (ARC) Foundation Models. arXiv:2508.06471 [cs.CL] <https://arxiv.org/abs/2508.06471>
- [60] Pei-Shuo Wang, Jian-Jia Chen, Chun-Che Yang, Chi-Chih Chang, Ning-Chi Huang, Mohamed S. Abdelfattah, and Kai-Chiang Wu. 2025. Speculate Deep and Accurate: Lossless and Training-Free Acceleration for Offloaded LLMs via Substitute Speculative Decoding. In *The Thirty-ninth Annual Conference on Neural Information Processing Systems*. <https://openreview.net/forum?id=ZDpPfg9pDc>
- [61] Wenfeng Wang, Jiacheng Liu, Xiaofeng Hou, Xinfeng Xia, Peng Tang, Mingxuan Zhang, Chao Li, and Minyi Guo. 2025. MoE-SpeQ: Speculative Quantized Decoding with Proactive Expert Prefetching and Offloading for Mixture-of-Experts. arXiv:2511.14102 [cs.LG] <https://arxiv.org/abs/2511.14102>
- [62] Yun Wang, Lingyun Yang, Senhao Yu, Yixiao Wang, Ruixing Li, Zhixiang Wei, James Yen, and Zhengwei Qi. 2025. BuddyMoE: Exploiting Expert Redundancy to Accelerate Memory-Constrained Mixture-of-Experts Inference. arXiv:2511.10054 [cs.LG] <https://arxiv.org/abs/2511.10054>
- [63] Tony F. Wu, Huichu Liu, H. Ekin Sumbul, Lita Yang, Dipti Baheti, Jeremy Coriell, William Koven, Anu Krishnan, Mohit Mittal, Matheus Trevisan Moreira, Max Waugaman, Laurent Ye, and Edith Beigné. 2024. 11.2 A 3D Integrated Prototype System-on-Chip for Augmented Reality Applications Using Face-to-Face Wafer Bonded 7nm Logic at  $< 2 \mu\text{m}$  Pitch with up to 40% Energy Reduction at Iso-Area Footprint. In *2024 IEEE International Solid-State Circuits Conference (ISSCC)*, Vol. 67. 210–212. <https://doi.org/10.1109/ISSCC49657.2024.10454529>
- [64] John Wu, Rahul Agarwal, Michael Ciraula, Carl Dietz, Brett Johnson, Dave Johnson, Russell Schreiber, Raja Swaminathan, Will Walker, and Samuel Naffziger. 2022. 3D V-Cache: the Implementation of a Hybrid-Bonded 64MB Stacked Cache for a 7nm x86-64 CPU. In *2022 IEEE International Solid-State Circuits Conference (ISSCC)*, Vol. 65. 428–429. <https://doi.org/10.1109/ISSCC42614.2022.9731565>
- [65] Leyang Xue, Yao Fu, Zhan Lu, Luo Mai, and Mahesh Marina. 2025. MoE-Infinity: Efficient MoE Inference on Personal Machines with Sparsity-Aware Expert Cache. arXiv:2401.14361 [cs.LG] <https://arxiv.org/abs/2401.14361>
- [66] An Yang, Anfeng Li, Baosong Yang, Beichen Zhang, Binyuan Hui, Bo Zheng, Bowen Yu, Chang Gao, Chengen Huang, Chenxu Lv, Chujie Zheng, Dayiheng Liu, Fan Zhou, Fei Huang, Feng Hu, Hao Ge, Haoran Wei, Huan Lin, Jialong Tang, Jian Yang, Jianhong Tu, Jianwei Zhang, Jianxin Yang, Jiayi Yang, Jing Zhou, Jingren Zhou, Junyang Lin, Kai Dang, Keqin Bao, Kexin Yang, Le Yu, Lianghao Deng, Mei Li, Mingfeng Xue, Mingze Li, Pei Zhang, Peng Wang, Qin Zhu, Rui Men, Ruize Gao, Shixuan Liu, Shuang Luo, Tianhao Li, Tianyi Tang, Wenbiao Yin, Xingzhang Ren, Xinyu Wang, Xinyu Zhang, Xuancheng Ren, Yang Fan, Yang Su, Yichang Zhang, Yinger Zhang, Yu Wan, Yuqiong Liu, Zekun Wang, Zeyu Cui, Zhenru Zhang, Zhipeng Zhou, and Zihan Qiu. 2025. Qwen3 Technical Report. arXiv:2505.09388 [cs.CL] <https://arxiv.org/abs/2505.09388>
- [67] Lita Yang, Kavya Sreedhar, Huichu Liu, and Edith Beigne. 2024. Enabling On-Device Large Language Models with 3D-Stacked Memory. In *NeurIPS 2024 Workshop Machine Learning with new Compute Paradigms*. <https://openreview.net/forum?id=P4LViaB8g0>
- [68] Yichao Yuan, Lin Ma, and Nishil Talati. 2025. MoE-Lens: Towards the Hardware Limit of High-Throughput MoE LLM Serving Under Resource Constraints. arXiv:2504.09345 [cs.DC] <https://arxiv.org/abs/2504.09345>
- [69] Zhiheng Yue, Huizheng Wang, Jiahao Fang, Jinyi Deng, Guangyuan Lu, Fengbin Tu, Ruiqi Guo, Yuxuan Li, Yubin Qin, Yang Wang, Chao Li, Huiming Han, Shaojun Wei, Yang Hu, and Shouyi Yin. 2025. Exploiting Similarity Opportunities of Emerging Vision AI Models on Hybrid Bonding Architecture. In *Proceedings of the 51st Annual International Symposium on Computer Architecture* (Buenos Aires, Argentina) (ISCA '24). IEEE Press, 396–409. <https://doi.org/10.1109/ISCA59077.2024.00037>
- [70] Sungmin Yun, Kwanhee Kyung, Juhwan Cho, Jaewan Choi, Jongmin Kim, Byeongho Kim, Sukhan Lee, Kyomin Sohn, and Jung Ho Ahn. 2024. Duplex: A Device for Large Language Models with Mixture of Experts, Grouped Query Attention, and Continuous Batching. In *2024 57th IEEE/ACM International Symposium on Microarchitecture (MICRO)*. 1429–1443. <https://doi.org/10.1109/MICRO61859.2024.00105>
- [71] Wentao Zhao, Boya Lv, Meng Wu, Peiyu Chen, Fengyun Yan, Yufei Ma, Tianyu Jia, Ru Huang, and Le Ye. 2025. 3D-TokSIM: Stacking 3D Memory with Token-Stationary Compute-in-Memory for Speculative LLM Inference. In *2025 62nd ACM/IEEE Design Automation Conference (DAC)*. 1–7. <https://doi.org/10.1109/DAC63849.2025.11132883>
- [72] Lianmin Zheng, Wei-Lin Chiang, Ying Sheng, Siyuan Zhuang, Zhanghao Wu, Yonghao Zhuang, Zi Lin, Zhuohan Li, Dacheng Li, Eric P. Xing, Hao Zhang, Joseph E. Gonzalez, and Ion Stoica. 2023. Judging LLM-as-a-judge with MT-bench and Chatbot Arena. In *Proceedings of the 37th International Conference on Neural Information Processing Systems* (New Orleans, LA, USA) (NIPS '23). Curran Associates Inc., Red Hook, NY, USA, Article 2020, 29 pages.